The scattering coefficients of superconducting microwave resonators: II. System-bath approach

Qi-Ming Chen,[1,2,*] Matti Partanen,[1] Florian Fesquet,[1,2] Kedar E. Honasoge,[1,2] Fabian Kronowetter,[1,2] Yuki Nojiri,[1,2] Michael Renger,[1,2] Kirill G. Fedorov,[1,2] Achim Marx,[1] Frank Deppe,[1,2,3,†] and Rudolf Gross[1,2,3,‡]

[1] *Walther-Meißner-Institut, Bayerische Akademie der Wissenschaften, 85748 Garching, Germany*
[2] *Physik-Department, Technische Universität München, 85748 Garching, Germany*
[3] *Munich Center for Quantum Science and Technology (MCQST), Schellingstr. 4, 80799 Munich, Germany*

(Dated: February 23, 2022)

We describe a unified quantum approach for analyzing the scattering coefficients of superconducting microwave resonators with a variety of geometries. We also generalize the method to a chain of resonators with time delays, and reveal several transport properties similar to a photonic crystal. It is shown that both the quantum and classical analyses provide consistent results, and they together reveal different decay and decoherence mechanisms in a general microwave resonator. These results form a solid basis for understanding the scattering spectrums of networks of microwave resonators, and pave the way for applying superconducting microwave resonators in complex circuits.

arXiv:2109.07766v2 [quant-ph] 22 Feb 2022

I. INTRODUCTION

Understanding the scattering coefficients of superconducting microwave resonators is crucial to the study of superconducting quantum circuits [1]. Owing to the high design flexibility and the strong interactions, a variety of novel photon transport properties emerge when coupling a microwave resonator to other circuit components [2–19]. For example, it is shown that a dissipative atom can completely reflect the photons propagating along a 1D waveguide with no loss [2–4], although the physical size of the atom is much smaller than the wavelength of the propagating microwave field. Moreover, microwave resonators can also be coupled to each other with different geometries, which lead to many interesting phenomena such as the Fano resonance [20–24], slow light [25–29], coupled-resonator-induced transparency [30–33], and localized bound states [34–40]. During the past decades, the scattering coefficients of superconducting quantum circuits have attracted an enormous interest and led to a variety of discoveries. However, most of the existing work either assume the input microwave field to be a few-photon Fock states [41] or consider a purely classical microwave field as the input [42]. Moreover, those proposed methods are often limited to certain scenarios without general applicability. For example, one often uses the transfer-matrix method to study a hanger-type resonator, but has to switch to the system-bath description to calculate the scattering coefficients of a necklace-type resonator [43, 44]. A unified approach that applies to a general superconducting microwave resonator is still missing, but it is in high-demand for design larger circuits.

Here, and also in a parallel paper [45], we study the scattering coefficients of superconducting microwave resonators in either quantum or classical perspectives. In this work, we employ the the system-bath method in quantum optics and derive the analytical descriptions of the scattering coefficients [46–48]. We compare the results with the classical approach [45], and reveal the correspondence of different concepts in the two languages, such as the the damping rates and the quality factors. We also generalize the method to a chain of microwave resonators, which form a photonic-crystal-like system and exhibit interesting transport features that are qualitatively different from a single resonator. These results provide a systematic study of the scattering coefficients of superconducting microwave resonators in the quantum perspective.

The rest of this paper is organized as follows: In Sec. II, we outline the system-bath method and derive the scattering coefficients of a single microwave resonator, which couples to the external circuity in various geometries. Next, we generalize our method to a chain of hanger-type resonators with time delay in Sec. III, which are side-coupled to an extended waveguide with different time delays. We also study a chain of necklace-type resonators in Sec. IV, which are coupled to each other through the ends. Finally, we conclude this study, compare the classical and quantum methods, and discuss how the dephasing effect can be incorporated in the analysis in Sec. V. Detailed derivations of the input-output relations and the scattering coefficients for resonators with different geometries can be found in Appendices A-D.

II. SCATTERING COEFFICIENTS OF A SINGLE MICROWAVE RESONATOR

A. The hanger-type $\lambda/4$ resonators

The hanger-type $\lambda/4$ resonator is schematically shown in Fig. 1(a)-(b), where the intra-resonator field, a, is coupled to the modes b of an waveguide with a coupling

* qiming.chen@wmi.badw.de
† frank.deppe@wmi.badw.de
‡ rudolf.gross@wmi.badw.de

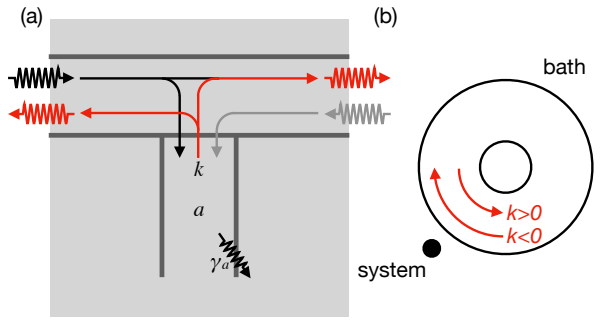


FIG. 1. Schematic of a hanger-type $\lambda/4$ resonator. Here, a short-circuited $\lambda/4$ (i.e., the system) is side-coupled to a transmission-line waveguide (i.e., the bath), which accommodates both left- and right-propagating fields. Panel (b) shows a simplified schematic of (a), where we describe the bath as a circular tube indicating the use of periodic boundary conditions.

strength κ. We describe the coupled system as

$$H_{\rm s} = \hbar\omega_0 a^\dagger a, \tag{1}$$

$$H_{\rm b} = \sum_{k=-\infty}^{+\infty} \hbar\omega_k b_k^\dagger b_k, \tag{2}$$

$$H_{\rm sb} = \sum_{k=-\infty}^{+\infty} \hbar\left(\kappa^* a b_k^\dagger + \kappa a^\dagger b_k\right). \tag{3}$$

Following the standard procedure of the input-output analysis [46, 47], which is also outlined in Appendix A, one can derive a set of linear equations that relate the dynamics of the intra-resonator field, a, to a bath of input and output fields, b. However, the input and output fields defined in this way are not directly related to the fields measured in experiments. To calculate the transport properties of the system, one must distinguish the left and the right propagating fields, which we denote as l and r, from the bath b, as shown in Fig. 1(b).

Keeping this in mind, we constrain our discussion to a small frequency interval around the central driving frequency, $\omega_{\rm d}$. Within this small interval we can approximate the dispersion by the linear relation [22]

$$\omega_k = \omega_{\rm d} \mp v_{\rm g}\delta_k. \tag{4}$$

Here, $v_{\rm g}$ is the group velocity of the waveguide, $\delta_k = k \pm k_{\rm d}$ with k and $k_{\rm d} > 0$ being the wave vectors that correspond to the frequencies ω_k and $\omega_{\rm d}$, respectively. In the rotating frame at $\omega_{\rm d}$, we obtain an equivalent description of the coupled system

$$H_{\rm s} = \hbar\left(\omega_0 - \omega_{\rm d}\right) a^\dagger a, \tag{5}$$

$$H_{\rm b} = \sum_{\Delta_k=-\infty}^{+\infty} \hbar v_{\rm g}\Delta_k \left(-l_{k_{\rm r}-\Delta_k}^\dagger l_{k_{\rm r}-\Delta_k} + r_{k_{\rm r}+\Delta_k}^\dagger r_{k_{\rm r}+\Delta_k}\right), \tag{6}$$

$$H_{\rm sb} = \sum_{\Delta_k=-\infty}^{+\infty} \hbar\left(\kappa^* a l_{k_{\rm r}-\Delta_k}^\dagger + \kappa a^\dagger l_{k_{\rm r}-\Delta_k} + \kappa^* a r_{k_{\rm r}+\Delta_k}^\dagger + \kappa a^\dagger r_{k_{\rm r}+\Delta_k}\right). \tag{7}$$

Here, we have extended the upper and lower limits of the summation to infinity for mathematical convenience, which is valid as long as $\omega_{\rm d}$ is much larger than the typical bandwidth of interest [41]. Finally, we complete our transformation by defining $\omega = v_{\rm g}\delta_k$, $\Delta_a = \omega_0 - \omega_{\rm d}$, and replacing the discrete field operators by a continuum: $l_{k_{\rm r}-\Delta_{\rm k}} \to l_\omega$, $r_{k_{\rm r}+\Delta_{\rm k}} \to r_\omega$. The result is

$$H_{\rm s} = \hbar\Delta_a a^\dagger a, \tag{8}$$

$$H_{\rm b} = \int_{-\infty}^{+\infty} d\omega\hbar\omega\left(-l_\omega^\dagger l_\omega + r_\omega^\dagger r_\omega\right), \tag{9}$$

$$H_{\rm sb} = \int_{-\infty}^{+\infty} d\omega\hbar\left(\kappa^* a l_\omega^\dagger + \kappa a^\dagger l_\omega + \kappa^* a r_\omega^\dagger + \kappa a^\dagger r_\omega\right). \tag{10}$$

By separating the left- and right-propagating fields in the waveguide, we split the original bath, b, into two independent baths, l and r, representing different directions of field propagation in the 1D waveguide. In this way, the scattering coefficients of the resonator can be readily obtained by following the standard input-output analysis. Here, we list several major steps for illustration. Using the Heisenberg equations of motion, we describe the dynamics of the intra-resonator field, a, and the two bath fields, l_ω and r_ω, as

$$\dot{a} = -i\Delta_a a - i\int_{-\infty}^{+\infty} d\omega\kappa\left(l_\omega + r_\omega\right), \tag{11}$$

$$\dot{l}_\omega = +i\omega l_\omega - i\kappa^* a, \tag{12}$$

$$\dot{r}_\omega = -i\omega r_\omega - i\kappa^* a. \tag{13}$$

We further define the input and output fields corresponding to the two baths as

$$l_{\rm in} = \frac{1}{\sqrt{2\pi}}\int_{-\infty}^{+\infty} d\omega e^{+i\omega t} l_\omega,\ l_{\rm out} = l_{\rm in} + \sqrt{\gamma}a, \tag{14}$$

$$r_{\rm in} = \frac{1}{\sqrt{2\pi}}\int_{-\infty}^{+\infty} d\omega e^{-i\omega t} r_\omega,\ r_{\rm out} = r_{\rm in} + \sqrt{\gamma}a, \tag{15}$$

where $\sqrt{\gamma} = i\sqrt{2\pi}\kappa$. Inserting Eqs. (14)-(15) into (11)-(13), we obtain

$$\dot{a} = -i\Delta_a a - \left(\gamma + \frac{\gamma_a}{2}\right)a - \sqrt{\gamma}\left(l_{\rm in} + r_{\rm in}\right). \tag{16}$$

Here, we have added the intrinsic damping of the resonator, $\gamma_a/2$, by hand.

Equations (14)-(15) and (16) determine the scattering coefficients of a hanger-type $\lambda/4$ resonator, which are defined as

$$S_{11} = \frac{\langle l_{\rm out}\rangle}{\langle r_{\rm in}\rangle},\ S_{21} = \frac{\langle r_{\rm out}\rangle}{\langle r_{\rm in}\rangle} \text{ with } \langle l_{\rm in}\rangle = 0, \tag{17}$$

$$S_{12} = \frac{\langle l_{\rm out}\rangle}{\langle l_{\rm in}\rangle},\ S_{22} = \frac{\langle r_{\rm out}\rangle}{\langle l_{\rm in}\rangle} \text{ with } \langle r_{\rm in}\rangle = 0. \tag{18}$$

That is,

$$S_{11} = S_{22} = -\frac{\gamma}{i\Delta_a + \left(\gamma + \frac{\gamma_a}{2}\right)}, \tag{19}$$

$$S_{21} = S_{12} = 1 - \frac{\gamma}{i\Delta_a + \left(\gamma + \frac{\gamma_a}{2}\right)}. \tag{20}$$

We recall that the scattering coefficients of a hanger-type $\lambda/4$ resonator which are derived by using the transfer-matrix approach are given by [45]

$$S_{11} = S_{22} \approx -\frac{\frac{\omega_a}{2Q_{\rm c}}}{i\Delta_a + \left(\frac{\omega_a}{2Q_{\rm i}} + \frac{\omega_a}{2Q_{\rm c}}\right)}, \tag{21}$$

$$S_{21} = S_{12} \approx 1 - \frac{\frac{\omega_a}{2Q_{\rm c}}}{i\Delta_a + \left(\frac{\omega_a}{2Q_{\rm i}} + \frac{\omega_a}{2Q_{\rm c}}\right)}. \tag{22}$$

Here, we have replaced the imaginary unit, j, that follows the convension of microwave engineering by the imaginary unit $i = -j$ [49]. Comparing Eqs. (19)-(20) with (21)-(22), we obtain the following relations between the damping rates and the quality factors:

$$\gamma_a = \frac{\omega_a}{Q_{\rm i}},\ \gamma = \frac{\omega_a}{2Q_{\rm c}}. \tag{23}$$

The above relation also holds for a hanger-type $\lambda/2$ resonator, but with different definitions of the resonant frequency and the quality factors. The physical interpretation of this result is obvious: First, if the coupling rate between the resonator and the waveguide vanishes ($\gamma \to 0$), the external quality factor diverges ($Q_c \to \infty$). Second, if the intrinsic decay rate of the resonator vanishes ($\gamma_a \to 0$), the internal quality factors diverges ($Q_i \to \infty$). We note that the factor of *two* in the expression of γ originates from the fact that both the left- and right-propagating fields in the waveguide couple to the intra-resonator field. However, the effective energy decay rate in both the internal and coupling dissipation channels equals to the ratio between the resonant frequency and the corresponding Q factor.

B. The necklace-type $\lambda/2$ resonator

The necklace-type $\lambda/2$ resonator is schematically shown in Fig. 2(a)-(b), where the intra-resonator field, a, is coupled to two independent baths, b_1 and b_2, on the left and right hand side, respectively. We describe the whole system as

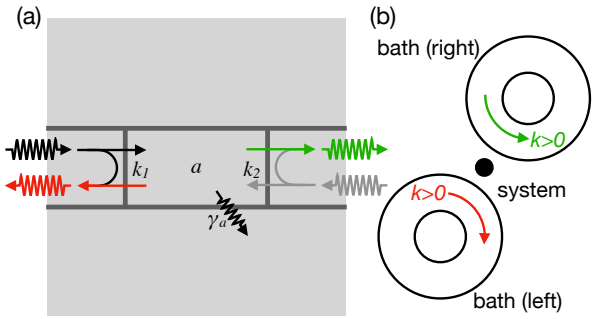


FIG. 2. Schematic of a necklace-type $\lambda/2$ resonator. Here, an open-circuited $\lambda/2$ (i.e., the system) is directly coupled to two transmission-line waveguides (i.e., the baths) at the two ends, respectively. Each of the bath accommodates only one unidirectional propagating field. We use different colors for the outgoing fields emitting to emphasize the π phase shift of the intra-resonator spatial mode at the two ends.

$$H_{\rm s} = \hbar\omega_{\rm d} a^\dagger a, \tag{24}$$

$$H_{\rm b} = \sum_{m=1}^{2}\sum_{k=0}^{+\infty} \hbar\omega_k b_{m,k}^\dagger b_{m,k}, \tag{25}$$

$$H_{\rm sb} = \sum_{m=1}^{2} (-1)^{m-1} \sum_{k=0}^{+\infty} \hbar\left(\kappa_m^* a b_{m,k}^\dagger + \kappa_m a^\dagger b_{m,k}\right). \tag{26}$$

Here, the wave vector, k, takes only positive values that defines a unidirectional propagation of the microwave fields in the two feedlines, as shown in Fig. 2(b). The phase factor ± 1 in the system-bath interaction takes into account the π phase difference of the spatial modes with $(2n+1)\lambda/2 = l$ at the two ends of the resonator, whereas there is no phase difference for the modes with $2n\lambda/2 = l$.

Following a similar procedure as before, we linearize the dispersion relation around the central driving frequency

$$\omega_k = \omega_{\rm d} + v_{\rm g}\Delta_k. \tag{27}$$

Eventually, we obtain the Hamiltonian in terms of photon frequencies

$$H_{\rm s} = \hbar\Delta_a a^\dagger a, \tag{28}$$

$$H_{\rm b} = \sum_{m=1}^{2}\int_{-\infty}^{+\infty} d\omega \hbar\omega b_{m,\omega}^\dagger b_{m,\omega}, \tag{29}$$

$$H_{\rm sb} = \sum_{m=1}^{2} (-1)^{m-1} \int_{-\infty}^{+\infty} d\omega\hbar\left(\kappa_m^* a b_{m,\omega}^\dagger + \kappa_m a^\dagger b_{m,\omega}\right). \tag{30}$$

By using the Heisenberg equations of motion, we describe the dynamics of the intra-resonator field, a, and the two

bath fields, $b_{1,\omega}$ and $b_{2,\omega}$, as

$$\dot{a} = -i\Delta_a a - i\sum_{m=1}^{2}(-1)^{m-1}\int_{-\infty}^{+\infty} d\omega \kappa_m b_{m,\omega}, \quad (31)$$

$$\dot{b}_{1,\omega} = -i\omega b_{1,\omega} - i\kappa_1^* a, \quad (32)$$

$$\dot{b}_{2,\omega} = -i\omega b_{2,\omega} + i\kappa_2^* a. \quad (33)$$

We further define the input and output fields corresponding to the two baths as

$$b_{1,\text{in}} = \frac{1}{\sqrt{2\pi}}\int_{-\infty}^{+\infty} d\omega e^{+i\omega t} b_{1,\omega},\ b_{1,\text{out}} = b_{1,\text{in}} + \sqrt{\gamma_1}a, \quad (34)$$

$$b_{2,\text{in}} = \frac{1}{\sqrt{2\pi}}\int_{-\infty}^{+\infty} d\omega e^{-i\omega t} b_{2,\omega},\ b_{2,\text{out}} = b_{2,\text{in}} - \sqrt{\gamma_2}a. \quad (35)$$

Inserting Eqs. (34)-(35) into (31)-(33), we obtain

$$\dot{a} = -i\Delta_a a - \left(\frac{\gamma_1+\gamma_2}{2} + \frac{\gamma_a}{2}\right)a + \sum_{m=1}^{2}(-1)^m\sqrt{\gamma_m}b_{m,\text{in}}. \quad (36)$$

Here, we have defined $\sqrt{\gamma_m} = i\sqrt{2\pi}\kappa_m$ and added the intrinsic damping of the resonator, $\gamma_a/2$, by hand.

Equations (34)-(35) and (36) determine the scattering coefficients of a necklace-type $\lambda/2$ resonator, which are defined as

$$S_{11} = \frac{\langle b_{1,\text{out}}\rangle}{\langle b_{1,\text{in}}\rangle},\ S_{21} = \frac{\langle b_{2,\text{out}}\rangle}{\langle b_{1,\text{in}}\rangle} \text{ with } \langle b_{2,\text{in}}\rangle = 0, \quad (37)$$

$$S_{12} = \frac{\langle b_{1,\text{out}}\rangle}{\langle b_{2,\text{in}}\rangle},\ S_{22} = \frac{\langle b_{2,\text{out}}\rangle}{\langle b_{2,\text{in}}\rangle} \text{ with }, \langle b_{1,\text{in}}\rangle = 0. \quad (38)$$

That is,

$$S_{11} = 1 - \frac{\gamma_1}{i\Delta_a + \left(\frac{\gamma_1+\gamma_b}{2} + \frac{\gamma_a}{2}\right)}, \quad (39)$$

$$S_{21} = S_{12} = \frac{\sqrt{\gamma_1\gamma_b}}{i\Delta_a + \left(\frac{\gamma_1+\gamma_b}{2} + \frac{\gamma_a}{2}\right)}, \quad (40)$$

$$S_{22} = 1 - \frac{\gamma_b}{i\Delta_a + \left(\frac{\gamma_1+\gamma_b}{2} + \frac{\gamma_a}{2}\right)}. \quad (41)$$

We recall that the scattering coefficients of a necklace-type $\lambda/2$ resonator which have been derived by using the transfer-matrix approach [45]

$$S_{11} \approx 1 - \frac{\frac{\omega_a}{Q_{c_1}}}{i\Delta_a + \left(\frac{\omega_a}{2Q_i} + \frac{\omega_a}{2Q_{c_1}} + \frac{\omega_a}{2Q_{c_2}}\right)}, \quad (42)$$

$$S_{21} = S_{12} \approx \frac{\frac{\omega_a}{\sqrt{Q_{c_1}Q_{c_2}}}}{i\Delta_a + \left(\frac{\omega_a}{2Q_i} + \frac{\omega_a}{2Q_{c_1}} + \frac{\omega_a}{2Q_{c_2}}\right)}, \quad (43)$$

$$S_{22} \approx 1 - \frac{\frac{\omega_a}{Q_{c_2}}}{i\Delta_a + \left(\frac{\omega_a}{2Q_i} + \frac{\omega_a}{2Q_{c_1}} + \frac{\omega_a}{2Q_{c_2}}\right)}. \quad (44)$$

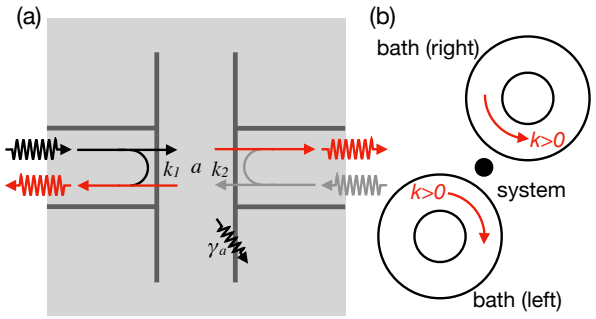


FIG. 3. Schematic of a bridge-type $\lambda/2$ resonator. Here, a short-circuited $\lambda/2$ (i.e., the system) is directly coupled to two transmission-line waveguides (i.e., the baths) at the same anti-node. Each of the bath accommodates only one unidirectional propagating field.

Comparing Eqs.(39)-(41), with (42)-(44), we obtain the following relations between the decay rates and the quality factos of a necklace-type $\lambda/2$ resonator

$$\gamma_a = \frac{\omega_a}{Q_i},\ \gamma_1 = \frac{\omega_a}{Q_{c_1}},\ \gamma_2 = \frac{\omega_a}{Q_{c_2}}, \quad (45)$$

which also hold for a necklace-type $\lambda/4$ resonator but with different definitions of the resonant frequency and the quality factors.

C. The bridge-type $\lambda/2$ resonators

The bridge-type $\lambda/2$ resonator is schematically shown in Fig. 3(a)-(b), where the intra-resonator field, a, is coupled to two independent baths, b_1 and b_2, on the left and right sides, respectively. Compared with the Hamiltonian for a necklace-type $\lambda/2$ resonator, the major difference lies in the system-bath interaction term

$$H_{\text{sb}} = \sum_{m=1}^{2}\sum_{k=0}^{+\infty}\hbar\left(\kappa_m^* a b_{m,k}^\dagger + \kappa_m a^\dagger b_{m,k}\right). \quad (46)$$

That is, we assume no phase difference in the system-bath interaction as the two baths are coupled to the resonator mode at the same voltage anti-node. Consequently, the input-output relations are also similar to that of the necklace-type $\lambda/2$ resonator

$$b_{1,\text{out}} = b_{1,\text{in}} + \sqrt{\gamma_1}a, \quad (47)$$

$$b_{2,\text{out}} = b_{2,\text{in}} + \sqrt{\gamma_2}a. \quad (48)$$

$$\dot{a} = -i\Delta_a a - \left(\frac{\gamma_1+\gamma_2}{2} + \frac{\gamma_a}{2}\right)a - \sum_{m=1}^{2}\sqrt{\gamma_m}b_{m,\text{in}}, \quad (49)$$

Here, we have also added the intrinsic damping of the resonator, $\gamma_a/2$, by hand. The scattering coefficients of

a bridge-type $\lambda/2$ resonator are

$$S_{11} = 1 - \frac{\gamma_1}{i\Delta_a + \left(\frac{\gamma_1+\gamma_b}{2} + \frac{\gamma_a}{2}\right)}, \tag{50}$$

$$S_{21} = S_{12} = -\frac{\sqrt{\gamma_1\gamma_b}}{i\Delta_a + \left(\frac{\gamma_1+\gamma_b}{2} + \frac{\gamma_a}{2}\right)}, \tag{51}$$

$$S_{22} = 1 - \frac{\gamma_b}{i\Delta_a + \left(\frac{\gamma_1+\gamma_b}{2} + \frac{\gamma_a}{2}\right)}. \tag{52}$$

We recall that the scattering coefficients of a bridge-type $\lambda/2$ resonator which have been derived by using the classical transfer-matrix approach [45]

$$S_{11} \approx 1 - \frac{\frac{\omega_a}{Q_{c_1}}}{i\Delta_a + \left(\frac{\omega_a}{2Q_i} + \frac{\omega_a}{2Q_{c_1}} + \frac{\omega_a}{2Q_{c_2}}\right)}, \tag{53}$$

$$S_{21} = S_{12} \approx \frac{\frac{\omega_a}{\sqrt{Q_{c_1}Q_{c_2}}}}{i\Delta_a + \left(\frac{\omega_a}{2Q_i} + \frac{\omega_a}{2Q_{c_1}} + \frac{\omega_a}{2Q_{c_2}}\right)}, \tag{54}$$

$$S_{22} \approx 1 - \frac{\frac{\omega_a}{Q_{c_2}}}{i\Delta_a + \left(\frac{\omega_a}{2Q_i} + \frac{\omega_a}{2Q_{c_1}} + \frac{\omega_a}{2Q_{c_2}}\right)}. \tag{55}$$

Comparing Eqs. (50)-(52) with (53)-(55), we obtain the following relations between the decay rates and the quality factos of a bridge-type $\lambda/2$ resonator

$$\gamma_a = \frac{\omega_a}{Q_i},\ \gamma_1 = \frac{\omega_a}{Q_{c_1}},\ \gamma_2 = \frac{\omega_a}{Q_{c_2}}. \tag{56}$$

As a final remark we emphasize that the system-bath method provides an elegant and unified approach for deriving the scattering coefficients of a general microwave resonator. Here, the key idea is to linearize the dispersion relation of the waveguide and transform the Hamiltonian from the wave vector space to the frequency space. This separation is natural for necklace- and bridge-type resonators with two spatially separated baths, and has been reported recently in the literature [43, 44]. However, it is not a trivial task to apply the method to a hanger-type resonator. Here, we artificially split the single physical bath into two baths with opposite signs of the wave vectors [22], and relate the scattering coefficients to these two new fields. Depending on the specific geometry of the system, the scattering coefficients can be readily obtained by taking the mean value of the field operators in Eqs. (17)-(18) for hanger-type resonators, or in Eqs. (37)-(38) for necklace- or bridge-type resonators.

III. COUPLING MULTIPLE HANGER-TYPE RESONATORS TO A LONG WAVEGUIDE

A. General scattering coefficients

Let us now consider a more complex system with N hanger-type resonators that are side-coupled to a long waveguide, as schematically shown in Fig. 4(a)-(b). The total Hamiltonian is

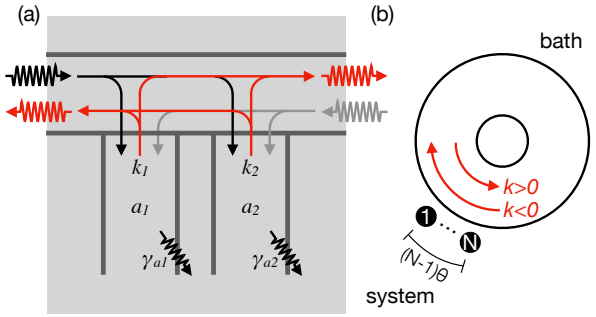


FIG. 4. Schematic of a chain of N hanger-type $\lambda/4$ resonators (i.e., the system) that are side-coupled to a long transmission-line waveguide (i.e., the bath). The bath accommodates both left- and right-propagating fields. We denote the time delay between a propagating photon and the different short-circuited $\lambda/4$ resonators as θ.

$$H_s = \sum_{j=1}^{N} \hbar\Delta_j a_j^\dagger(t) a_j(t), \tag{57}$$

$$H_b = \int_{-\infty}^{+\infty} d\omega\hbar\omega \left[-l_\omega^\dagger(t) l_\omega(t) + r_\omega^\dagger(t) r_\omega(t)\right], \tag{58}$$

$$H_{sb} = \sum_{j=1}^{N} \int_{-\infty}^{+\infty} d\omega\hbar \Big\{ e^{-i(j-1)\omega\tau} \kappa_j^* a_j(t) l_\omega^\dagger \left[t - (j-1)\tau\right] + \kappa_j^* a_j(t) r_\omega^\dagger \left[t - (j-1)\tau\right] + \text{c.c.} \Big\}. \tag{59}$$

Here, we explicitly included the phase differences $\theta_j = (j-1)\omega\tau = (j-1)\theta$ in the interaction between the bath fields, l_ω and r_ω, and the different resonators, a_j, which are coupled to the waveguide at different positions labelled by j. Following the derivations in Appendix B, we obtain the following relation that describes the evolution of the intra-resonator field

$$\dot{a}_j = -i\omega_j a_j - \frac{\gamma_{a_j}}{2} a_j - \sum_{j'=1}^{N} \sqrt{\gamma_j} \left(\sqrt{\gamma_{j'}}\right)^* e^{|j'-j|\theta} a_{j'}(t) - \sqrt{\gamma_j} l_{\text{in}}(t)\, e^{-i(j-N)\theta} - \sqrt{\gamma_j} r_{\text{in}}(t)\, e^{i(j-1)\theta}. \tag{60}$$

Here, $\theta = \omega_d\tau$, with ω_d being the central driving frequency, is the phase difference in the coupling rate between two neighboring resonators, and τ the time delay of the propagating field traveling between the finite distance between them. The operators, l_{in} and r_{in}, are respectively defined as the input fields at the right and left hand side of the waveguide, which propagate in opposite directions, as shown in Fig. 4(b). Correspondingly, we define l_{out} and r_{out} as the output fields at the left and right hand side of the waveguide,

respectively

$$l_{\rm out} = e^{i(N-1)\theta} l_{\rm in} + \sum_{j'=1}^{N} \left(\sqrt{\gamma_{j'}}\right)^* e^{i(j'-1)\theta} a_j, \qquad (61)$$

$$r_{\rm out} = e^{i(N-1)\theta} r_{\rm in} + \sum_{j'=1}^{N} \left(\sqrt{\gamma_{j'}}\right)^* e^{i(N-j')\theta} a_j. \qquad (62)$$

With these results, the scattering coefficients of the whole system can be readily obtained by using the expression in Eqs. (17)-(18). For example, for the simplest case with $N = 2$ we have

$$S_{11} = -\frac{\gamma_1 (i\Delta_2 + \gamma_{a_2}) + e^{i2\theta}\gamma_2 (i\Delta_1 + \gamma_{a_1}) + \gamma_1\gamma_2 \left(1 - e^{i2\theta}\right)}{(i\Delta_1 + \gamma_{a_1})(i\Delta_2 + \gamma_{a_2}) + \gamma_1 (i\Delta_2 + \gamma_{a_2}) + \gamma_2 (i\Delta_1 + \gamma_{a_1}) + \gamma_1\gamma_2 (1 - e^{i2\theta})}, \qquad (63)$$

$$S_{21} = S_{12} = \frac{e^{i\theta} (i\Delta_1 + \gamma_{a_1})(i\Delta_2 + \gamma_{a_2})}{(i\Delta_1 + \gamma_{a_1})(i\Delta_2 + \gamma_{a_2}) + \gamma_1 (i\Delta_2 + \gamma_{a_2}) + \gamma_2 (i\Delta_1 + \gamma_{a_1}) + \gamma_1\gamma_2 (1 - e^{i2\theta})}, \qquad (64)$$

$$S_{22} = -\frac{e^{i2\theta}\gamma_1 (i\Delta_2 + \gamma_{a_2}) + \gamma_2 (i\Delta_1 + \gamma_{a_1}) + \gamma_1\gamma_2 \left(1 - e^{i2\theta}\right)}{(i\Delta_1 + \gamma_{a_1})(i\Delta_2 + \gamma_{a_2}) + \gamma_1 (i\Delta_2 + \gamma_{a_2}) + \gamma_2 (i\Delta_1 + \gamma_{a_1}) + \gamma_1\gamma_2 (1 - e^{i2\theta})}, \qquad (65)$$

$$(66)$$

This result is equivalent to that reported in Refs. 20 and 23, but with different methods in the derivation.

B. Simulation results

For large N, it is rather tedious to derive an analytical expression of the scattering coefficients and it may be even cumbersome to do numerical simulations. Fortunately, efficient algorithms exist if we simplify the discussion to $\Delta_j \equiv \Delta$, $g_j \equiv g$, and $\gamma_{a_j} \equiv \gamma_a$, as shown in Appendix C. Here, we perform several numerical simulations for cross checking the results derived above. We choose the real propagating constant $\alpha = 5.0 \times 10^{-3}$ /m, phase velocity $v_{\rm p} = 1.35 \times 10^8$ m/s, the coupling capacitor $C = 1.0 \times 10^{-14}$ F, and the resonator length $l = 5 \times 10^{-3}$ m for each $\lambda/4$ resonator. The resonant frequency of each individual resonator is estimated to be $\omega_{\rm r} = 2\pi \times 6.659$ GHz, with the external and internal decay rates of the resonator, $\gamma = 2\pi \times 928$ kHz and $\gamma_a = 2\pi \times 212$ kHz [45].

In Fig. 5(a), we vary the phase difference, θ, i.e. the distance between neighboring resonators, and calculate the scattering coefficients for $N = 2$. On the one hand, the absolute value of the reflection and transmission amplitudes exhibit an asymmetric Fano resonance line shape for $\theta \neq n\pi/2$ with $n = 0, 1, \cdots$ [23]. Depending on whether $\theta = n\pi$ or $n\pi + \pi/2$, we obtain a symmetric Lorentzian spectrum, which is also known as the Breit-Wigner resonance [50], or a symmetric Fano spectrum [51], respectively. These line shapes can be better seen in Fig. 5(d), where we fix θ to several values. On the other hand, a transition between the symmetric and asymmetric line spectra occurs at $\theta = n\pi/2$. As can bee seen in the corresponding phase diagrams, the transition is smooth at $\theta = n\pi$. However, an abrupt π phase shift happens for every $\theta = n\pi + \pi/2$, which distinguishes the symmetric Lorentzian spectrum from the symmetric Fano spectrum . With the increase of N, the transition between symmetric and asymmetric line shapes emerge more frequently and occur at $\theta = n\pi + 2n'\pi/2^N$ for $n = 0, 1, \cdots$ and $n' = 1, \cdots, n-1$, as shown in Fig. 5(a)-(c). Correspondingly, the sudden π phase change happens at $\theta = (2n+1)\pi/2^N$.

We also compare the reflection line shape for different N and θ in Fig. 5(d). It can be clearly seen that the phase factor, θ, determines whether a broadening or narrowing of the spectrum is to be observed with an increasing N. For example, the full width at half maximum (FWHM) increases moronically with N for $\theta = 0$, or equivalently 2π, while it decreases moronically for $\theta = \pi/2$. These observations indicate that, by coupling multiple hanger-type resonators evenly alongside a waveguide, one can engineer the scattering coefficients of the system and obtain a photonic crystal microwave resonator as a whole. Depending on the parameter θ, the new resonator can have a huge enhancement or reduction of the Q factors compared with each individual hanger-type resonator, which provides a new freedom to the resonator design in superconducting quantum circuits.

IV. COUPLING MULTIPLE NECKLACE-TYPE RESONATORS IN A CHAIN

A. General scattering coefficients

Let us now consider a system with N necklace-type resonators coupled to each other in a linear chain, as schematically shown in Fig. 6(a)-(b). The total

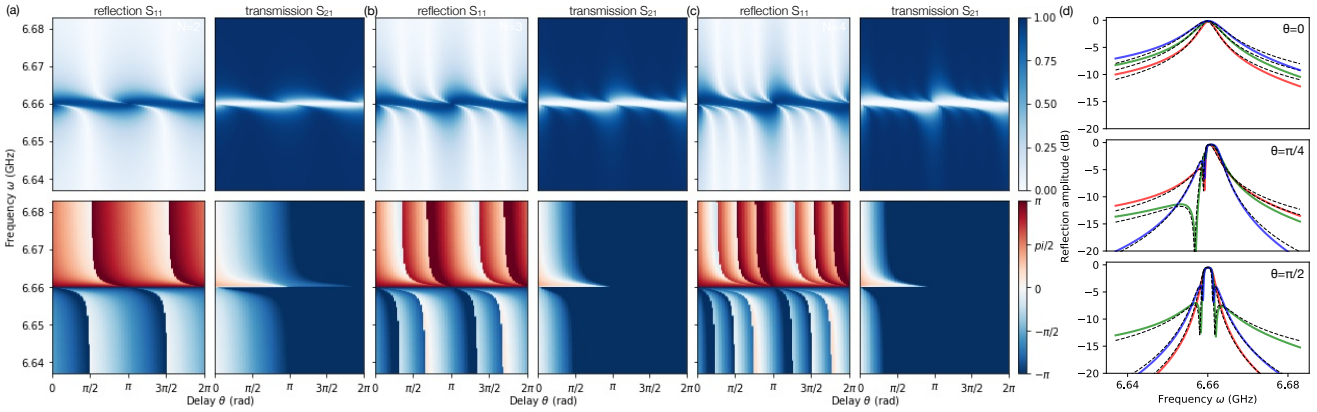


FIG. 5. scattering coefficients of a chain of N hanger-type $\lambda/4$ resonators which are coupled to an extended waveguide. (a) For $N = 2$, the spectrum periodically changes from a symmetric to an asymmetric line shape with the increase of θ. The symmetric line shapes are obtained at $\theta = n\pi/2$, while there exits a sudden π phase change for every $\theta = n\pi + \pi/2$. (b)-(c) With the increase of N, the switch becomes more frequently in θ. Here, sudden π phase changes occur at $\theta = (2n+1)\pi/2^N$ for $n = 1, \cdots, N-1$. (d) The reflection responses for $\theta = 0, \pi/4, \pi/2$ (top, middle,bottom) and $N = 2, 3, 4$ (red, green, blue). The black dashed curves indicate the results derived in the system-bath approach. The resonant frequency ω_0 is calculated by using the method introduced in Ref. [45], which is shifted by 1 MHz for a better fitting.

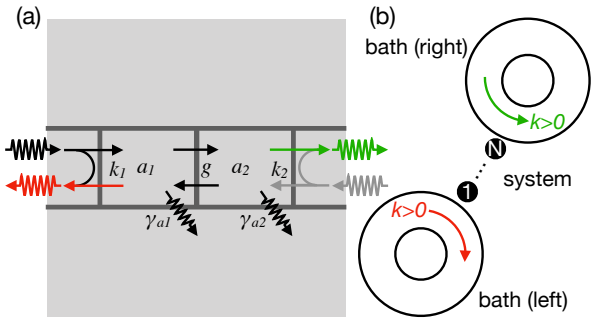


FIG. 6. Schematic of a chain of coupled necklace-type $\lambda/2$ resonators (i.e., the system), which is coupled to two transmission-line waveguides (i.e., the baths) at the two ends, respectively. Each of the bath accommodates only one unidirectional propagating field. We also use different colors for the outgoing fields emitting to emphasize the π phase shift of the intra-resonator spatial mode at the two ends.

Hamiltonian reads as

$$H_{\rm s} = \sum_{j=1}^{N} \hbar\Delta_j a_j^\dagger a_j - \sum_{j=1}^{N-1} \hbar g_j \left(a_j^\dagger a_{j+1} + a_j a_{j+1}^\dagger\right), \quad (67)$$

$$H_{\rm b} = \sum_{m=1}^{2} \int_{-\infty}^{+\infty} d\omega \hbar\omega b_{m,\omega}^\dagger b_{m,\omega}, \quad (68)$$

$$H_{\rm sb} = \int_{-\infty}^{+\infty} d\omega \hbar \left(\kappa_1^* a_1 b_{1,\omega}^\dagger + \kappa_1 a_1^\dagger b_{1,\omega} - \kappa_2^* a_N b_{2,\omega}^\dagger - \kappa_2 a_N^\dagger b_{2,\omega}\right). \quad (69)$$

The input-output relations can be readily obtained by following the standard procedure

$$b_{1,\rm out} = b_{1,\rm in} + \sqrt{\gamma_1} a_1, \quad (70)$$

$$b_{2,\rm out} = b_{2,\rm in} - \sqrt{\gamma_2} a_N, \quad (71)$$

and, in turn, the evolution of the intra-resonator reads

$$\dot{a}_j = \begin{cases} -i\Delta_1 a_1 + ig_1 a_2 - \left(\frac{\gamma_1}{2} + \frac{\gamma_{a_1}}{2}\right) a_1 - \sqrt{\gamma_1} b_{1,\rm in}, & \text{for } j = 1; \\ -i\Delta_j a_j + i\left(g_{j-1} a_{j-1} + g_j a_{j+1}\right) - \frac{\gamma_{a_j}}{2} a_j, & \text{for } 1 < j < N; \\ -i\Delta_N a_N + ig_{N-1} a_{N-1} - \left(\frac{\gamma_2}{2} + \frac{\gamma_{a_N}}{2}\right) a_N + \sqrt{\gamma_2} b_{2,\rm in}, & \text{for } j = N. \end{cases} \quad (72)$$

Similar to the single-resonator case, the scattering coefficients can be obtained by finding the mean-field steady-state solution of Eqs. (70)-(72). For example, for the simplest case with $N = 2$, we have

$$S_{11} = 1 - \frac{\gamma_1 \left[i\Delta_2 + \left(\frac{\gamma_2}{2} + \frac{\gamma_{a_2}}{2}\right)\right]}{\left[i\Delta_1 + \left(\frac{\gamma_1}{2} + \frac{\gamma_{a_1}}{2}\right)\right]\left[i\Delta_2 + \left(\frac{\gamma_2}{2} + \frac{\gamma_{a_2}}{2}\right)\right] + g^2}, \quad (73)$$

$$S_{21} = S_{12} = \frac{-ig\sqrt{\gamma_1\gamma_2}}{\left[i\Delta_1 + \left(\frac{\gamma_1}{2} + \frac{\gamma_{a_1}}{2}\right)\right]\left[i\Delta_2 + \left(\frac{\gamma_2}{2} + \frac{\gamma_{a_2}}{2}\right)\right] + g^2}, \quad (74)$$

$$S_{22} = 1 - \frac{\gamma_2 \left[i\Delta_1 + \left(\frac{\gamma_1}{2} + \frac{\gamma_{a_1}}{2}\right)\right]}{\left[i\Delta_1 + \left(\frac{\gamma_1}{2} + \frac{\gamma_{a_1}}{2}\right)\right]\left[i\Delta_2 + \left(\frac{\gamma_2}{2} + \frac{\gamma_{a_2}}{2}\right)\right] + g^2}. \quad (75)$$

This result has been derived and experimentally demonstrated in our previous work [52].

B. The tight-binding model

To gain further physical insight beyond the numerical solutions for large N, we further assume that $\Delta_j \equiv \Delta$, $g_j \equiv g$, and $\gamma_{a_j} \equiv \gamma_a$, such that the resonator chain can be described by a bosonic tight-binding model. For a finite number of resonators, N, we define the following collective modes of the resonator chain

$$a_k = \sum_{j=1}^{N} \sqrt{\frac{2}{N+1}} \sin\left(\frac{\pi k j}{N+1}\right) a_j. \tag{76}$$

This replacement of variable is similar to the definition of magnon in spin systems [53]. In this way, we can rewrite Eqs. (70)-(72) in a more compact form

$$l_{\text{out}} = l_{\text{in}} + \sum_{k=1}^{N} \sqrt{\gamma_{1,k}} a_k, \tag{77}$$

$$r_{\text{out}} = r_{\text{in}} + \sum_{k=1}^{N} (-1)^k \sqrt{\gamma_{2,k}} a_k, \tag{78}$$

$$\begin{aligned} \dot{a}_k = &-\left(i\Delta_k + \frac{\gamma_a}{2}\right) a_k - \left[\sqrt{\gamma_{1,k}} b_{1,\text{in}} + (-1)^k \sqrt{\gamma_{2,k}} b_{2,\text{in}}\right] \\ &- \frac{1}{2} \sum_{k'=1}^{N} \left[\sqrt{\gamma_{1,k}\gamma_{1,k'}} + (-1)^{k+k'} \sqrt{\gamma_{2,k}\gamma_{2,k'}}\right] a_{k'}. \end{aligned} \tag{79}$$

Here, $\Delta_k = \Delta - 2g\cos\left(\frac{k\pi}{N+1}\right)$, $\sqrt{\gamma_{m,k}} = \sqrt{2\gamma_m/(N+1)}\sin\left[k\pi/(N+1)\right]$. With these results, one can readily obtain the following analytical expressions for the scattering coefficients (see Appendix D for detail)

$$S_{11} = 1 - \frac{\left[\left(1 + \frac{1}{2}\sum_{k=1}^{N} \frac{\gamma_{2,k}}{i\Delta_k + \frac{\gamma_a}{2}}\right)\left(\sum_{k=1}^{N} \frac{\gamma_{1,k}}{i\Delta_k + \frac{\gamma_a}{2}}\right) - \frac{1}{2}\left(\sum_{k=1}^{N} \frac{(-1)^k \sqrt{\gamma_{1,k}\gamma_{2,k}}}{i\Delta_k + \frac{\gamma_a}{2}}\right)^2\right]}{\left(1 + \frac{1}{2}\sum_{k=1}^{N} \frac{\gamma_{1,k}}{i\Delta_k + \frac{\gamma_a}{2}}\right)\left(1 + \frac{1}{2}\sum_{k=1}^{N} \frac{\gamma_{2,k}}{i\Delta_k + \frac{\gamma_a}{2}}\right) - \left(\frac{1}{2}\sum_{k=1}^{N} \frac{(-1)^k \sqrt{\gamma_{1,k}\gamma_{2,k}}}{i\Delta_k + \frac{\gamma_a}{2}}\right)^2}, \tag{80}$$

$$S_{21} = S_{12} = -\frac{\left(\sum_{k=1}^{N} \frac{(-1)^k \sqrt{\gamma_{1,k}\gamma_{2,k}}}{i\Delta_k + \frac{\gamma_a}{2}}\right)}{\left(1 + \frac{1}{2}\sum_{k=1}^{N} \frac{\gamma_{1,k}}{i\Delta_k + \frac{\gamma_a}{2}}\right)\left(1 + \frac{1}{2}\sum_{k=1}^{N} \frac{\gamma_{2,k}}{i\Delta_k + \frac{\gamma_a}{2}}\right) - \left(\frac{1}{2}\sum_{k=1}^{N} \frac{(-1)^k \sqrt{\gamma_{1,k}\gamma_{2,k}}}{i\Delta_k + \frac{\gamma_a}{2}}\right)^2}, \tag{81}$$

$$S_{22} = 1 - \frac{\left[\left(1 + \frac{1}{2}\sum_{k=1}^{N} \frac{\gamma_{1,k}}{i\Delta_k + \frac{\gamma_a}{2}}\right)\left(\sum_{k=1}^{N} \frac{\gamma_{2,k}}{i\Delta_k + \frac{\gamma_a}{2}}\right) - \frac{1}{2}\left(\sum_{k=1}^{N} \frac{(-1)^k \sqrt{\gamma_{1,k}\gamma_{2,k}}}{i\Delta_k + \frac{\gamma_a}{2}}\right)^2\right]}{\left(1 + \frac{1}{2}\sum_{k=1}^{N} \frac{\gamma_{1,k}}{i\Delta_k + \frac{\gamma_a}{2}}\right)\left(1 + \frac{1}{2}\sum_{k=1}^{N} \frac{\gamma_{2,k}}{i\Delta_k + \frac{\gamma_a}{2}}\right) - \left(\frac{1}{2}\sum_{k=1}^{N} \frac{(-1)^k \sqrt{\gamma_{1,k}\gamma_{2,k}}}{i\Delta_k + \frac{\gamma_a}{2}}\right)^2}. \tag{82}$$

We note that the replacement of variables in Eq. (76) is valid for a linear chain of a finite number of microwave resonators. However, one may also assume a periodic boundary condition which describes a N-resonator loop or an infinitly long chain of resonators with $N \to \infty$

$$a_k = \sum_{j=1}^{N} \sqrt{\frac{1}{N}} \exp\left(\frac{i2\pi k j}{N}\right) a_j. \tag{83}$$

This replacement leads to a slightly different dispersive relation $\Delta_k = \Delta - 2g\cos(2k\pi/N)$, and the damping rates $\sqrt{\gamma_{1,k}} = \sqrt{\gamma_1/N}\exp\left[-i2\pi k/N\right]$, $\sqrt{\gamma_{2,k}} = \sqrt{\gamma_2/N}$. The input-output relations are

$$l_{\text{out}} = l_{\text{in}} + \sum_{k=1}^{N} \sqrt{\gamma_{1,k}} a_k, \tag{84}$$

$$r_{\text{out}} = r_{\text{in}} - \sum_{k=1}^{N} \sqrt{\gamma_{2,k}} a_k, \tag{85}$$

$$\begin{aligned} \dot{a}_k = &-\left(i\Delta_k + \frac{\gamma_a}{2}\right) a_k - \left[\sqrt{\gamma_{1,k}} b_{1,\text{in}} - \sqrt{\gamma_{2,k}} b_{2,\text{in}}\right] \\ &- \frac{1}{2} \sum_{k'=1}^{N} \left[\sqrt{\gamma_{1,k}\gamma_{1,k'}} + \sqrt{\gamma_{2,k}\gamma_{2,k'}}\right] a_{k'}, \end{aligned} \tag{86}$$

and the scattering parameters can be expressed as

$$S_{11} = 1 - \frac{\left[\left(1+\frac{1}{2}\sum_{k=1}^{N}\frac{\gamma_{1,k}}{i\Delta_k+\frac{\gamma_a}{2}}\right)\left(\sum_{k=1}^{N}\frac{\gamma_{1,k}}{i\Delta_k+\frac{\gamma_a}{2}}\right)-\frac{1}{2}\left(\sum_{k=1}^{N}\frac{\sqrt{\gamma_{1,k}\gamma_{2,k}}}{i\Delta_k+\frac{\gamma_a}{2}}\right)^2\right]}{\left(1+\frac{1}{2}\sum_{k=1}^{N}\frac{\gamma_{1,k}}{i\Delta_k+\frac{\gamma_a}{2}}\right)\left(1+\frac{1}{2}\sum_{k=1}^{N}\frac{\gamma_{2,k}}{i\Delta_k+\frac{\gamma_a}{2}}\right)-\left(\frac{1}{2}\sum_{k=1}^{N}\frac{\sqrt{\gamma_{1,k}\gamma_{2,k}}}{i\Delta_k+\frac{\gamma_a}{2}}\right)^2}, \tag{87}$$

$$S_{21} = S_{12} = \frac{\left(\sum_{k=1}^{N}\frac{\sqrt{\gamma_{1,k}\gamma_{2,k}}}{i\Delta_k+\frac{\gamma_a}{2}}\right)}{\left(1+\frac{1}{2}\sum_{k=1}^{N}\frac{\gamma_{1,k}}{i\Delta_k+\frac{\gamma_a}{2}}\right)\left(1+\frac{1}{2}\sum_{k=1}^{N}\frac{\gamma_{2,k}}{i\Delta_k+\frac{\gamma_a}{2}}\right)-\left(\frac{1}{2}\sum_{k=1}^{N}\frac{\sqrt{\gamma_{1,k}\gamma_{2,k}}}{i\Delta_k+\frac{\gamma_a}{2}}\right)^2}, \tag{88}$$

$$S_{22} = 1 - \frac{\left[\left(1+\frac{1}{2}\sum_{k=1}^{N}\frac{\gamma_{1,k}}{i\Delta_k+\frac{\gamma_a}{2}}\right)\left(\sum_{k=1}^{N}\frac{\gamma_{2,k}}{i\Delta_k+\frac{\gamma_a}{2}}\right)-\frac{1}{2}\left(\sum_{k=1}^{N}\frac{\sqrt{\gamma_{1,k}\gamma_{2,k}}}{i\Delta_k+\frac{\gamma_a}{2}}\right)^2\right]}{\left(1+\frac{1}{2}\sum_{k=1}^{N}\frac{\gamma_{1,k}}{i\Delta_k+\frac{\gamma_a}{2}}\right)\left(1+\frac{1}{2}\sum_{k=1}^{N}\frac{\gamma_{2,k}}{i\Delta_k+\frac{\gamma_a}{2}}\right)-\left(\frac{1}{2}\sum_{k=1}^{N}\frac{\sqrt{\gamma_{1,k}\gamma_{2,k}}}{i\Delta_k+\frac{\gamma_a}{2}}\right)^2}. \tag{89}$$

C. Simulation results

As a crosscheck of the results derived above, we performed several numerical simulations with the same parameters as before. However, the resonator length should be extended to $l = 10\times10^{-3}\,\mathrm{m}$ for $\lambda/2$ resonators. For each individual resonator, the resonant frequency is estimated to be $\omega_\mathrm{r} = 2\pi \times 6.659\,\mathrm{GHz}$. The decay rates are $\gamma = 2\pi \times 1.86\,\mathrm{MHz}$ and $\gamma_a = 2\pi \times 212\,\mathrm{kHz}$.

In Fig. 5(a), we calculate the scattering coefficients for increasing N. On the one hand, we observe that the number of resonant frequencies in the spectrum increases with the number of resonators. On the other hand, the spread of the resonant frequencies of the whole system also scales with N but saturates to a finite value. The bandwidth is approximately four times of the coupling strength, $g \approx 2\pi \times 44\,\mathrm{MHz}$, which is calculated by using the method introduced in Ref. [45]. This phenomena can be readily understood in the dispersion relation of the collective fields a_k. A more detailed inspection of the spectrum around ω_r indicates that the photons at the central resonant frequency can be almost fully transmitted or reflected, depending on whether there is an *odd* or *even* number of resonators in the chain, as shown in Fig. 5(b). This observation indicates a possible application that a chain of coupled resonators can be used as a single-photon switch [54, 55]. Moreover, we observe that the FWHM of the line shape decreases monotonically with N, as shown in Figs. 5(c). It indicates the existence of high Q-factor mode in an array of coupled resonators, which has been theoretically predicted by using the transfer-matrix method and experimentally demonstrated in the literature [26, 56–58]. Together with the result of a chain of hanger-type resonators, we conclude that coupling multiple microwave resonators can fundamentally change the scattering coefficients of the system and provide a novel way to increase the Q factors of superconducting microwave resonators.

V. CONCLUSIONS AND OUTLOOK

In conclusion, we provide a systematic study of the scattering coefficients of superconducting microwave resonators in the quantum perspective. By transforming the Hamiltonian from the wave vector space to the frequency space, we describe a unified approach for input-output analysis that applies to a general microwave resonator. The corresponding scattering coefficients are consistent with those derived in the classical transfer-matrix approach [45]. We also generalize our method to more complex systems with multiple hanger- or necklace-type resonators and time delays. We reveal several interesting photon transport phenomena in such photonic-crystal-like systems and find consistency with the results reported in the literature.

Compared with the transfer-matrix approach, the system-bath method has the advantage of simplicity which requires no detailed information of the circuit parameters. In this regard, it is more suitable to use the quantum approach to analyze the scattering coefficients of a complex circuit. However, the classical approach is more close to a physical system, which directly relates the electrical properties of a resonator, such as resonant frequency and quality factors, to the circuit parameters such as the coupling capacitance and the characteristic impedance. Nevertheless, a full description of a network of superconducting microwave resonators can be obtained by using either of the two approaches. They together provide a firm ground for the study of transport properties in a general superconducting quantum circuit.

As a closing remark, we note that dephasing of microwave resonators can also be incorporated in this theoretical frame, which is, however, often neglected in the literature. To describe dephasing, we write the

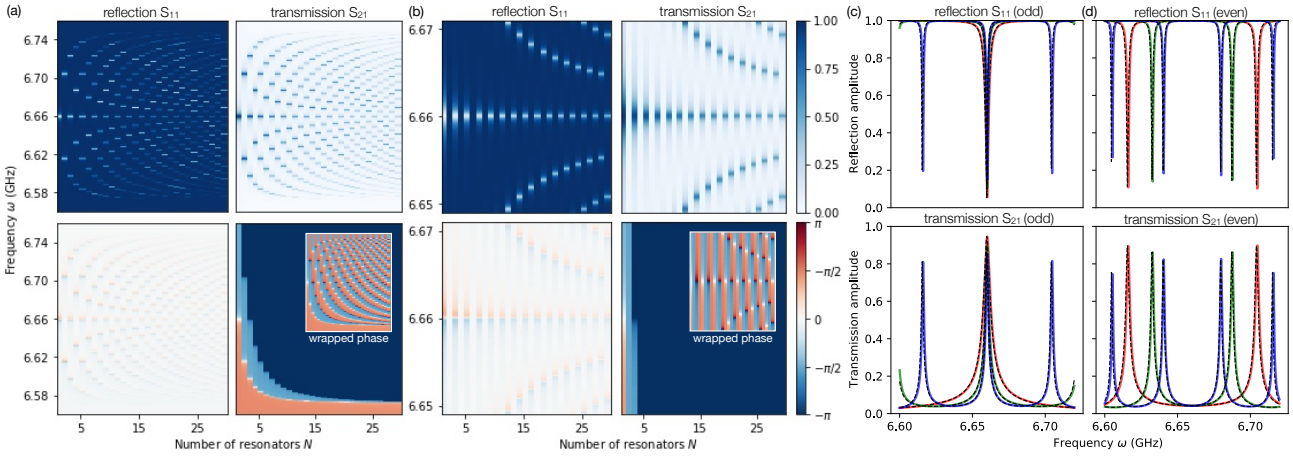


FIG. 7. scattering coefficients of a chain of coupled necklace-type $\lambda/4$ resonators, which couple to two feedlines at the ends. (a) With the increase of the resonator number, N, there emerges the same number of resonance dips or peak in the reflection and transmission responses. The spread of the peaks (dips) saturates at a value which equals to four times of the coupling strength. (b) A closer inspection of the spectrum around the central resonant frequency indicate that the incident photons can be almost fully reflected or transmitted depending on the parity of N. The FWHM of the central peak also decreases moronically with N. (c) The reflection and transmission responses for $N = 2, 3, 4$ (red, green, blue), respectively. The black dashed curves indicate the results derived in the system-bath approach. The resonant frequency ω_0 is calculated by using the method introduced in Ref. [45], which is shifted by 1 MHz for a better fitting.

system-bath interaction in the following form [59–63]

$$H_{\rm sb} = \sum_{m=1}^{2} (-1)^{m-1} \int_{-\infty}^{+\infty} d\omega \hbar a^\dagger a \left(\kappa_\phi^* b_{m,\omega}^\dagger + \kappa_\phi b_{m,\omega}\right). \tag{90}$$

The resulting input-output relation can be readily derived by following the same procedure as described above. The result is

$$\dot{a} = -i\Delta_a a - \frac{\gamma_\phi}{2} a - \sqrt{\gamma_\phi}\left(a b_{\rm in} - b_{\rm in}^\dagger a\right), \tag{91}$$

where $\sqrt{\gamma_\phi} = i\sqrt{2\pi}\kappa_\phi$. We note that the input field, $b_{\rm in} = \int_{-\infty}^{+\infty} d\omega e^{+i\omega t} b_\omega(0)/\sqrt{2\pi}$, does not commute with the intra-resonator field. However, the combined operator $b_{\rm in} + \left(\sqrt{\gamma_\phi}\right)^* a^\dagger a/2$ and $b_{\rm in}^\dagger + \sqrt{\gamma_\phi} a^\dagger a/2$ commute with all the system operators [60], such that we rewrite Eq. (91) as

$$\dot{a} = -i\Delta_a a - \sqrt{\gamma_\phi} a\left(b_{\rm in} - b_{\rm in}^\dagger\right). \tag{92}$$

This result indicates that the input field b causes a random jittering in the resonant frequency of the intra-resonator field, a. Even though it conserves the energy of the system, the dephasing effect broadens the line shape of the scattering responses such that one may not simply extract the energy dissipation rate from the measured FWHM of scattering spectrum. In this regard, one should resort to an extra measurement, for example, Ramsey interferometry, to distinguish the contributions of energy decay and dephasing in the FWHM. Today, high quality microwave resonators with $Q_{\rm i} > 10^6$ can be routinely made in lab [64]. We anticipate that a careful calibration and analysis of the dephasing rate may pave a significant step towards making even higher-quality superconducting microwave resonators in the near future.

ACKNOWLEDGMENTS

We acknowledge support by German Research Foundation via Germany's Excellence Strategy (EXC-2111-390814868), Elite Network of Bavaria through the program ExQM, European Union via the Quantum Flagship project QMiCS (No. 820505), German Federal Ministry of Education and Research via the project QuaRaTe (No. 13N15380).

Appendix A: Outline of the input-output analysis

We model a microwave resonator of any type as a composite system which the following Hamiltonian [47, 65]

$$H_{\rm s} = \sum_n \hbar\omega_n a_n^\dagger a_n, \tag{A1}$$

$$H_{\rm b} = \sum_m \hbar \int_{-\infty}^{+\infty} d\omega \omega b_{m,\omega}^\dagger b_{m,\omega}, \tag{A2}$$

$$H_{\rm sb} = \sum_{m,n} \hbar \int_{-\infty}^{+\infty} d\omega \left[\kappa_{m,n}^* a_n b_{m,\omega}^\dagger + \kappa_{m,n} a_n^\dagger b_{m,\omega}\right]. \tag{A3}$$

Following the Heisenberg equation, the time evolution of the intra-resonator field, a, as well as the bath field, b_ω, can be readily written as

$$\dot{a}_n = -i\omega_n a_n - i\sum_m \int_{-\infty}^{+\infty} d\omega \kappa_{m,n} l_m, \tag{A4}$$

$$\dot{l}_m = -i\omega l_m - i\sum_n \kappa_{m,n}^* a_n. \tag{A5}$$

By inserting the formal solution of Eq. (A5),

$$b_{m,\omega}(t) = e^{-i\omega(t-t_0)} b_{m,\omega}(t_0) - i\sum_n \kappa_{m,n'}^* \int_{t_0}^{t} dt' e^{-i\omega(t-t')} a_{n'}(t'). \tag{A6}$$

into Eq. (A4), we obtain

$$\dot{a}_n = -i\omega_n a_n - i\sum_m \kappa_{m,n} \int_{-\infty}^{+\infty} d\omega e^{-i\omega(t-t_0)} b_{m,\omega}(t_0) - \sum_{m,n'} \kappa_{m,n}\kappa_{m,n'}^* \int_{-\infty}^{+\infty} d\omega \int_{t_0}^{t} dt' e^{-i\omega(t-t')} a_{n'}(t') \tag{A7}$$

We recall the property

$$\int_{-\infty}^{+\infty} d\omega e^{-i\omega(t-t_0)} = 2\pi\delta(t-t_0) \tag{A8}$$

and defined the input field, i.e., the noise operator in quantum Langevin equation, as

$$b_{m,\rm in} = \frac{1}{\sqrt{2\pi}} \int_{-\infty}^{+\infty} d\omega e^{-i\omega(t-t_0)} b_{m,\omega}(t_0), \tag{A9}$$

the above equation can be simplified as

$$\dot{a}_n = -i\omega_n a_n - i\sum_m \sqrt{2\pi}\kappa_{m,n} b_{m,\rm in} - \sum_{m,n'} \pi\kappa_{m,n}\kappa_{m,n'}^* a_{n'}. \tag{A10}$$

Alternatively, the formal solution of Eq. (A5) may be written as

$$b_{m,\omega}(t) = e^{-i\omega(t-t_1)} b_{m,\omega}(t_1) + i\sum_n \kappa_{m,n'}^* \int_{t}^{t_1} dt' e^{-i\omega(t-t')} a_{n'}(t'). \tag{A11}$$

We have

$$\dot{a}_n = -i\omega_n a_n - i\sum_m \kappa_{m,n} \int_{-\infty}^{+\infty} d\omega e^{-i\omega(t-t_1)} b_{m,\omega}(t_1) + \sum_{m,n'} \kappa_{m,n}\kappa_{m,n'}^* \int_{-\infty}^{+\infty} d\omega \int_{t}^{t_1} dt' e^{-i\omega(t-t')} a_{n'} \tag{A12}$$

We defined the output field as

$$b_{m,\rm out} = \frac{1}{\sqrt{2\pi}} \int_{-\infty}^{+\infty} d\omega e^{-i\omega(t-t_1)} b_{m,\omega}(t_0), \tag{A13}$$

such that the above equation can be simplified as

$$\dot{a}_n = -i\omega_n a_n - i\sum_m \sqrt{2\pi}\kappa_{m,n} b_{m,\text{out}} + \sum_{m,n'} \pi\kappa_{m,n}\kappa^*_{m,n'} a_{n'}. \tag{A14}$$

Combining Eqs. (A9)-(A10) and (A13)-(A14), we obtain the so-called input-output analysis

$$\dot{a}_n = -i\omega_n a_n - \sum_m \sqrt{\gamma_{m,n}} b_{m,\text{in}} - \frac{1}{2}\sum_{m,n'} \sqrt{\gamma_{m,n}} \left(\sqrt{\gamma_{m,n'}}\right)^* a_{n'} - \frac{\gamma_{a_n}}{2} a_n, \tag{A15}$$

$$b_{m,\text{out}} = b_{m,\text{in}} + \sum_{n'} \left(\sqrt{\gamma_{m,n'}}\right)^* a_{n'}., \tag{A16}$$

Here, we have defined $\sqrt{\gamma_{m,n}} = i\sqrt{2\pi}\kappa_{m,n}$ and $\left(\sqrt{\gamma_{m,n}}\right)^* = -i\sqrt{2\pi}\kappa^*_{m,n}$ and add the intrinsic damping of the oscillator by hand.

Appendix B: A chain of hanger-type resonators with delays

We consider a composite system where N hanger-type resonators are side-coupled to a 1D waveguide. The system-bath interaction reads

$$H_{\text{sb}} = \sum_{j=1}^{N} \int_{-\infty}^{+\infty} d\omega\hbar \left\{ e^{-i(j-1)\omega\tau}\kappa^*_j a_j l^\dagger_\omega + e^{i(j-1)\omega\tau}\kappa_j a^\dagger_j l_\omega + e^{-i(j-1)\omega\tau}\kappa^*_j a_j r^\dagger_\omega + e^{i(j-1)\omega\tau}\kappa_j a^\dagger_j r_\omega \right\}. \tag{B1}$$

Here, we encode the information of the distance between different hanger-type resonators into a phase delay $l_\omega \to e^{i(j-1)\omega\tau} l_\omega$, $r_\omega \to e^{i(j-1)\omega\tau} r_\omega$, $j = 1, \cdots, N$. Following the same procedure in Appendix A, we describe the dynamics of the intra-resonator field, a_j, and the two bath fields, l_ω and r_ω, as

$$l_\omega(t) = e^{+i\omega(t-t_0)} l_\omega(t_0) - i\sum_n e^{-i(j-1)\omega\tau}\kappa^*_{m,n'} \int_{t_0}^{t} dt' e^{+i\omega(t-t')} a_{n'}(t'), \tag{B2}$$

$$r_\omega(t) = e^{-i\omega(t-t_0)} r_\omega(t_0) - i\sum_n e^{-i(j-1)\omega\tau}\kappa^*_{m,n'} \int_{t_0}^{t} dt' e^{-i\omega(t-t')} a_{n'}(t'). \tag{B3}$$

$$\begin{aligned}\dot{a}_j = &-i\omega_j a_j - i\kappa_j \int_{-\infty}^{+\infty} d\omega e^{+i\omega(t-t_0)} e^{i(j-1)\omega\tau} l_\omega(t_0) - \sum_{j'} \kappa_j\kappa^*_{j'} \int_{-\infty}^{+\infty} d\omega \int_{t_0}^{t} dt' e^{+i\omega(t-t')} e^{i(j-j')\omega\tau} a_{n'}(t') \\ &- i\kappa_j \int_{-\infty}^{+\infty} d\omega e^{-i\omega(t-t_0)} e^{-i(j-1)\omega\tau} r_\omega(t_0) - \sum_{j'} \kappa_j\kappa^*_{j'} \int_{-\infty}^{+\infty} d\omega \int_{t_0}^{t} dt' e^{-i\omega(t-t')} e^{i(j-j')\omega\tau} a_{n'}(t')\end{aligned} \tag{B4}$$

We define the input fields $l_{\text{in}} = \left(1/\sqrt{2\pi}\right) \int_{-\infty}^{+\infty} e^{+i\omega(t-t_0)} l_\omega(t_0) d\omega$, $r_{\text{in}} = \left(1/\sqrt{2\pi}\right) \int_{-\infty}^{+\infty} e^{+i\omega(t-t_0)} r_\omega(t_0) d\omega$, such that Eq. (B4) can be written in a compact form

$$\begin{aligned}\dot{a}_j = &-i\omega_j a_j - 2\pi\kappa_j\kappa^*_j a_j - i\sqrt{2\pi}\kappa_j l_{\text{in}}\left(t + (j-1)\tau\right) - i\sqrt{2\pi}\kappa_j r_{\text{in}}\left(t - (j-1)\tau\right) \\ &- 2\pi\sum_{j'>j} \kappa_j\kappa^*_{j'} a_{j'}\left[t + (j-j')\tau\right] - 2\pi\sum_{j'<j} \kappa_j\kappa^*_{j'} a_{j'}\left[t + (j'-j)\tau\right]\end{aligned} \tag{B5}$$

Here, a technical problem emerges that the time evolution of a_j involves operators at different times. To eliminate the time dependance of τ, we note that the above discussion is performed in the rotating frame at the driving frequency ω_{d}. Thus, a time delay of τ in the operators may be fairly approximated by a phase factor $\exp(i\theta)$ with $\theta = \omega_{\text{d}}\tau$. In this regard, we rewrite Eq. (B5) as

$$\begin{aligned}\dot{a}_j = &-i\omega_j a_j - 2\pi\kappa_j\kappa^*_j a_j - i\sqrt{2\pi}\kappa_j l_{\text{in}}(t)\, e^{-i(j-1)\theta} - i\sqrt{2\pi}\kappa_j r_{\text{in}}(t)\, e^{i(j-1)\theta} \\ &- 2\pi\sum_{j'>j} \kappa_j\kappa^*_{j'} e^{(j'-j)\theta} a_{j'}(t) - 2\pi\sum_{j'<j} \kappa_j\kappa^*_{j'} e^{(j-j')\theta} a_{j'}(t)\end{aligned} \tag{B6}$$

On the other hand, we have

$$l_\omega(t) = e^{+i\omega(t-t_1)} l_\omega(t_1) + i\sum_n e^{-i(j-1)\omega\tau}\kappa^*_{m,n'}\int_t^{t_1} dt' e^{+i\omega(t-t')} a_{n'}(t'), \tag{B7}$$

$$r_\omega(t) = e^{-i\omega(t-t_1)} r_\omega(t_1) + i\sum_n e^{-i(j-1)\omega\tau}\kappa^*_{m,n'}\int_t^{t_1} dt' e^{-i\omega(t-t')} a_{n'}(t'). \tag{B8}$$

$$\begin{aligned}\dot{a}_j = &-i\omega_j a_j - i\kappa_j\int_{-\infty}^{+\infty} d\omega e^{+i\omega(t-t_1)} e^{i(j-1)\omega\tau} l_\omega(t_1) + \sum_{j'}\kappa_j\kappa^*_{j'}\int_{-\infty}^{+\infty} d\omega\int_t^{t_1} dt' e^{+i\omega(t-t')} e^{i(j-j')\omega\tau} a_{n'}(t') \\ &- i\kappa_j\int_{-\infty}^{+\infty} d\omega e^{-i\omega(t-t_1)} e^{-i(j-1)\omega\tau} r_\omega(t_1) + \sum_{j'}\kappa_j\kappa^*_{j'}\int_{-\infty}^{+\infty} d\omega\int_t^{t_1} dt' e^{-i\omega(t-t')} e^{i(j-j')\omega\tau} a_{n'}(t')\end{aligned} \tag{B9}$$

We define the output fields $l_{\text{out}} = \left(1/\sqrt{2\pi}\right)\int_{-\infty}^{+\infty} e^{+i\omega(t-t_1)} l_\omega(t_1) d\omega$, $r_{\text{out}} = \left(1/\sqrt{2\pi}\right)\int_{-\infty}^{+\infty} e^{+i\omega(t-t_1)} r_\omega(t_1) d\omega$, and obtain

$$\begin{aligned}\dot{a}_j = &-i\omega_j a_j + 2\pi\kappa_j\kappa^*_j a_j - i\sqrt{2\pi}\kappa_j l_{\text{out}}(t) e^{-i(j-1)\theta} - i\sqrt{2\pi}\kappa_j r_{\text{out}}(t) e^{i(j-1)\theta} \\ &+ 2\pi\sum_{j'<j}\kappa_j\kappa^*_{j'} e^{(j'-j)\theta} a_{j'}(t) + 2\pi\sum_{j'>j}\kappa_j\kappa^*_{j'} e^{(j-j')\theta} a_{j'}(t).\end{aligned} \tag{B10}$$

Combining Eqs. (B6) and (B10), we obtain the input-output relations

$$l_{\text{out}} = l_{\text{in}} + \sqrt{2\pi}\kappa^*_{j'}\sum_{j'=1}^{N} e^{i(j'-1)\theta} a_j, \tag{B11}$$

$$r_{\text{out}} = r_{\text{in}} + \sqrt{2\pi}\kappa^*_{j'}\sum_{j'=1}^{N} e^{i(1-j')\theta} a_j. \tag{B12}$$

We note that the definition of input and output fields are different from that in Section. III. To get the exact form, we respectively redefine the operators l_{in} and r_{in} as the input fields at the right and left side of the waveguide, and l_{out} and r_{out} as the output fields at the left and right sides of the waveguide. In other words, we perform the transform $l_{\text{in}} \to e^{i(N-1)\theta} l_{\text{in}}$, $r_{\text{out}} \to e^{-i(N-1)\theta} r_{\text{out}}$. The new input-output relations are

$$\dot{a}_j = -i\omega_j a_j - 2\pi\sum_{j'=1}^{N}\kappa_j\kappa^*_{j'} e^{i|j'-j|\theta} a_{j'}(t) - i\sqrt{2\pi}\kappa_j l_{\text{in}}(t) e^{-i(j-N)\theta} - i\sqrt{2\pi}\kappa_j r_{\text{in}}(t) e^{i(j-1)\theta}, \tag{B13}$$

$$l_{\text{out}} = e^{i(N-1)\theta} l_{\text{in}} + \sum_{j'=1}^{N}\left(\sqrt{\gamma_{j'}}\right)^* e^{i(j'-1)\theta} a_j, \tag{B14}$$

$$r_{\text{out}} = e^{i(N-1)\theta} r_{\text{in}} + \sum_{j'=1}^{N}\left(\sqrt{\gamma_{j'}}\right)^* e^{i(N-j')\theta} a_j. \tag{B15}$$

Correspondingly, the scattering coefficients reads

$$S_{11} = \frac{\langle l_{\text{out}}\rangle}{\langle r_{\text{in}}\rangle},\ S_{21} = \frac{\langle r_{\text{out}}\rangle}{\langle r_{\text{in}}\rangle} \text{ with } \langle l_{\text{in}}\rangle = 0, \text{ and } S_{12} = \frac{\langle l_{\text{out}}\rangle}{\langle l_{\text{in}}\rangle},\ S_{22} = \frac{\langle r_{\text{out}}\rangle}{\langle l_{\text{in}}\rangle} \text{ with } \langle r_{\text{in}}\rangle = 0. \tag{B16}$$

For the simplicity of calculation, we define

$$c_j = \sum_{j'\geq j}\left(\sqrt{\gamma_{j'}}\right)^* e^{ij'\theta} a_{j'},\ d_j = \sum_{j'\leq j}\left(\sqrt{\gamma_{j'}}\right)^* e^{-ij'\theta} a_{j'}, \tag{B17}$$

such that the input-output relation can be written in a compact form

$$l_{\text{out}} = e^{i(N-1)\theta} l_{\text{in}} + e^{-i\theta} c_1, \tag{B18}$$

$$r_{\text{out}} = e^{i(N-1)\theta} r_{\text{in}} + e^{-i\theta} d_N. \tag{B19}$$

On the other hand, the steady-state solution of intra-resonator field, a_j, reads

$$\left(i\omega_j-\gamma_j+\frac{\gamma_{a_j}}{2}\right)a_j=-e^{-ij\theta}\sqrt{\gamma_j}c_j-e^{+ij\theta}\sqrt{\gamma_j}d_j-\sqrt{\gamma_j}l_{\text{in}}\left(t\right)e^{-i(j-N)\theta}-\sqrt{\gamma_j}r_{\text{in}}\left(t\right)e^{i(j-1)\theta}, \tag{B20}$$

and thus

$$c_j=\sum_{j'\geq j}-\frac{\gamma_{j'}}{i\omega_{j'}-\gamma_{j'}+\frac{\gamma_{a_{j'}}}{2}}\left(c_{j'}+e^{+i2j'\theta}d_{j'}+e^{+iN\theta}l_{\text{in}}+e^{i(2j'-1)\theta}r_{\text{in}}\right), \tag{B21}$$

$$d_j=\sum_{j'\leq j}-\frac{\gamma_{j'}}{i\omega_{j'}-\gamma_{j'}+\frac{\gamma_{a_{j'}}}{2}}\left(e^{-i2j'\theta}c_{j'}+d_{j'}+e^{+i(N-2j')\theta}l_{\text{in}}+e^{-i\theta}r_{\text{in}}\right). \tag{B22}$$

In these regards, one can readily obtain the input-output relations by solving a linear equation.

Appendix C: Numerical solution for a homogeneous hanger-type-resonator chain

Let us now derive an analytical expression for the scattering coefficients for the special case where $\gamma_j\equiv\gamma$, $\gamma_{a_j}\equiv\gamma_a$, $\Delta_k\equiv\Delta$. We define

$$c_j=\sum_{j'\geq j}\left(\sqrt{\gamma_{j'}}\right)^*e^{ij'\theta}a_{j'},\ d_j=\sum_{j'\leq j}\left(\sqrt{\gamma_{j'}}\right)^*e^{-ij'\theta}a_{j'}, \tag{C1}$$

such that the steady-state solution of Eq. (B20) can be written as

$$a_j=-\frac{e^{-ij\theta}\sqrt{\gamma_j}}{i\omega_j-\gamma_j+\frac{\gamma_{a_j}}{2}}c_j-\frac{e^{+ij\theta}\sqrt{\gamma_j}}{i\omega_j-\gamma_j+\frac{\gamma_{a_j}}{2}}d_j-\frac{e^{-i(j-N)\theta}\sqrt{\gamma_j}}{i\omega_j-\gamma_j+\frac{\gamma_{a_j}}{2}}l_{\text{in}}-\frac{e^{i(j-1)\theta}\sqrt{\gamma_j}}{i\omega_j-\gamma_j+\frac{\gamma_{a_j}}{2}}r_{\text{in}}. \tag{C2}$$

For convenience, we define $x=\gamma/\left(i\omega-\gamma+\gamma_a/2\right)$. By combing Eqs. (C1) and (C2), we obtain a set of linear equations

$$xe^{-i2\theta}c_1+\left(x+1\right)d_1+x\left(e^{+i(N-2)\theta}l_{\text{in}}+e^{-i\theta}r_{\text{in}}\right)=0, \tag{C3}$$

$$xe^{-i2(j+1)\theta}c_{j+1}-d_j+\left(x+1\right)d_{j+1}+x\left(e^{+i(N-2(j+1))\theta}l_{\text{in}}+e^{-i\theta}r_{\text{in}}\right)=0, \tag{C4}$$

$$\left(x+1\right)c_j-c_{j+1}+xe^{+i2j\theta}d_j+x\left(e^{+iN\theta}l_{\text{in}}+e^{i(2j-1)\theta}r_{\text{in}}\right)=0, \tag{C5}$$

$$\left(x+1\right)c_N+xe^{+i2N\theta}d_N+x\left(e^{+iN\theta}l_{\text{in}}+e^{i(2N-1)\theta}r_{\text{in}}\right)=0. \tag{C6}$$

Next, we decouple the variables c_j and d_j and obtain the following two sets of linear equations

$$-\frac{\left(1+2x\right)}{x}c_1+\frac{\left(1+x\right)}{x}c_2-e^{iN\theta}l_{\text{in}}-e^{i\theta}r_{\text{in}}=0, \tag{C7}$$

$$\frac{\left(x+1\right)e^{i2\theta}}{x}c_{j-1}-\frac{\left(1+2x+e^{i2\theta}\right)}{x}c_j+\frac{\left(1+x\right)}{x}c_{j+1}+e^{iN\theta}\left(e^{i2\theta}-1\right)l_{\text{in}}=0,\ j=2,\cdots,N-1, \tag{C8}$$

$$\frac{\left(x+1\right)e^{i2\theta}}{x}c_{N-1}-\frac{\left(1+2x+e^{i2\theta}\right)}{x}c_N+e^{iN\theta}\left(e^{i2\theta}-1\right)l_{\text{in}}=0. \tag{C9}$$

$$-\frac{\left(1+e^{i2\theta}+2x\right)}{x}d_1+\frac{e^{i2\theta}\left(x+1\right)}{x}d_2+\left(e^{i\theta}-e^{-i\theta}\right)r_{\text{in}}=0, \tag{C10}$$

$$\frac{\left(1+x\right)}{x}d_{j-1}-\frac{\left(1+e^{i2\theta}+2x\right)}{x}d_j+\frac{e^{i2\theta}\left(x+1\right)}{x}d_{j+1}+\left(e^{i\theta}-e^{-i\theta}\right)r_{\text{in}}=0,\ j=2,\cdots,N-1, \tag{C11}$$

$$\frac{\left(1+x\right)}{x}d_{N-1}-\frac{\left(1+2x\right)}{x}d_N-e^{-iN\theta}l_{\text{in}}-e^{-i\theta}r_{\text{in}}=0. \tag{C12}$$

The above equations consist of tridiagonal matrices, which can be efficiently solved by using the so-called Thomas or TDMA algorithm. That is $c_N=b'_N$, $c_j=b'_j-a'_jc_{j+1}$ for $j=N-1,\cdots,1$, where

$$a'_j=\begin{cases}-\frac{1+x}{1+2x},\ j=1,\\ -\frac{1+x}{\left(1+2x+e^{i2\theta}\right)+a'_{j-1}\left(1+x\right)e^{i2\theta}},\ j=2,\cdots,N-1,\end{cases}\quad,\ b'_j=\begin{cases}-\frac{x\left(e^{iN\theta}l_{\text{in}}+e^{i\theta}r_{\text{in}}\right)}{1+2x},\ j=1,\\ -\frac{xe^{iN\theta}\left(1-e^{i2\theta}\right)l_{\text{in}}-b'_{j-1}\left(1+x\right)e^{i2\theta}}{\left(1+2x+e^{i2\theta}\right)+a'_{j-1}\left(1+x\right)e^{i2\theta}},\ j=2,\cdots,N-1.\end{cases} \tag{C13}$$

Or, $d_1 = b'_N$, $d_{N-j+1} = b'_j - a'_j d_{N-j}$ for $j = N-1, \cdots, 1$, where

$$a'_j = \begin{cases} -\frac{1+x}{1+2x}, \, j = 1, \\ -\frac{1+x}{(1+2x+e^{i2\theta})+a'_{j-1}(1+x)e^{i2\theta}}, \, j = 2, \cdots, N-1, \end{cases} , \, b'_j = \begin{cases} -\frac{x\left(e^{-iN\theta}l_{\rm in}+e^{-i\theta}r_{\rm in}\right)}{1+2x}, \, j = 1, \\ -\frac{x\left(e^{-i\theta}-e^{i\theta}\right)r_{\rm in}-b'_{j-1}(1+x)e^{i2\theta}}{(1+2x+e^{i2\theta})+a'_{j-1}(1+x)e^{i2\theta}}, \, j = 2, \cdots, N-1 \end{cases} \tag{C14}$$

Appendix D: A chain of necklace-type resonators with two boundary conditions

For hard-wall boundary conditions, we define

$$c_1 = \sum_{k'=1}^{N} \sqrt{\gamma_{1,k'}} a_{k'}, \; c_2 = \sum_{k'=1}^{N} (-1)^{k'} \sqrt{\gamma_{2,k'}} a_{k'}, \tag{D1}$$

such that

$$a_k = -\frac{\frac{1}{2}\sqrt{\gamma_{1,k}} c_1 + \frac{(-1)^k}{2}\sqrt{\gamma_{2,k}} c_2 + \sqrt{\gamma_{1,k}} b_{1,\rm in} + (-1)^k \sqrt{\gamma_{2,k}} b_{2,\rm in}}{i\Delta_k + \frac{\gamma_a}{2}}. \tag{D2}$$

Combing Eqs. (D1) and (D2), we obtain

$$c_1 = -\sum_{k=1}^{N} \frac{\frac{1}{2}\gamma_{1,k} c_1 + \frac{(-1)^k}{2}\sqrt{\gamma_{1,k}\gamma_{2,k}} c_2 + \gamma_{1,k} b_{1,\rm in} + (-1)^k \sqrt{\gamma_{1,k}\gamma_{2,k}} b_{2,\rm in}}{i\Delta_k + \frac{\gamma_a}{2}}, \tag{D3}$$

$$c_2 = -\sum_{k=1}^{N} \frac{\frac{(-1)^k}{2}\sqrt{\gamma_{1,k}\gamma_{2,k}} c_1 + \frac{1}{2}\gamma_{2,k} c_2 + (-1)^k \sqrt{\gamma_{1,k}\gamma_{2,k}} b_{1,\rm in} + \gamma_{2,k} b_{2,\rm in}}{i\Delta_k + \frac{\gamma_a}{2}}. \tag{D4}$$

The solutions of c_1 and c_2 reads

$$c_1 = -\frac{\left[\left(1+\frac{1}{2}\sum_{k=1}^{N}\frac{\gamma_{2,k}}{i\Delta_k+\frac{\gamma_a}{2}}\right)\left(\sum_{k=1}^{N}\frac{\gamma_{1,k}}{i\Delta_k+\frac{\gamma_a}{2}}\right) - \frac{1}{2}\left(\sum_{k=1}^{N}\frac{(-1)^k\sqrt{\gamma_{1,k}\gamma_{2,k}}}{i\Delta_k+\frac{\gamma_a}{2}}\right)^2\right] b_{1,\rm in} + \left(\sum_{k=1}^{N}\frac{(-1)^k\sqrt{\gamma_{1,k}\gamma_{2,k}}}{i\Delta_k+\frac{\gamma_a}{2}}\right) b_{2,\rm in}}{\left(1+\frac{1}{2}\sum_{k=1}^{N}\frac{\gamma_{1,k}}{i\Delta_k+\frac{\gamma_a}{2}}\right)\left(1+\frac{1}{2}\sum_{k=1}^{N}\frac{\gamma_{2,k}}{i\Delta_k+\frac{\gamma_a}{2}}\right) - \left(\frac{1}{2}\sum_{k=1}^{N}\frac{(-1)^k\sqrt{\gamma_{1,k}\gamma_{2,k}}}{i\Delta_k+\frac{\gamma_a}{2}}\right)^2}, \tag{D5}$$

$$c_2 = -\frac{\left(\sum_{k=1}^{N}\frac{(-1)^k\sqrt{\gamma_{1,k}\gamma_{2,k}}}{i\Delta_k+\frac{\gamma_a}{2}}\right) b_{1,\rm in} + \left[\left(1+\frac{1}{2}\sum_{k=1}^{N}\frac{\gamma_{1,k}}{i\Delta_k+\frac{\gamma_a}{2}}\right)\left(\sum_{k=1}^{N}\frac{\gamma_{2,k}}{i\Delta_k+\frac{\gamma_a}{2}}\right) - \frac{1}{2}\left(\sum_{k=1}^{N}\frac{(-1)^k\sqrt{\gamma_{1,k}\gamma_{2,k}}}{i\Delta_k+\frac{\gamma_a}{2}}\right)^2\right] b_{2,\rm in}}{\left(1+\frac{1}{2}\sum_{k=1}^{N}\frac{\gamma_{1,k}}{i\Delta_k+\frac{\gamma_a}{2}}\right)\left(1+\frac{1}{2}\sum_{k=1}^{N}\frac{\gamma_{2,k}}{i\Delta_k+\frac{\gamma_a}{2}}\right) - \left(\frac{1}{2}\sum_{k=1}^{N}\frac{(-1)^k\sqrt{\gamma_{1,k}\gamma_{2,k}}}{i\Delta_k+\frac{\gamma_a}{2}}\right)^2}. \tag{D6}$$

Thus, the input-output relations can be readily obtained by inserting c_1 and c_2 into Eqs. (A15)-(A16).

For periodic boundary conditions, we define

$$c_1 = \sum_{k'=1}^{N} \sqrt{\gamma_{1,k'}} a_{k'}, \; c_2 = -\sum_{k'=1}^{N} \sqrt{\gamma_{2,k'}} a_{k'}, \tag{D7}$$

such that

$$a_k = -\frac{\frac{1}{2}\sqrt{\gamma_{1,k}} c_1 - \frac{1}{2}\sqrt{\gamma_{2,k}} c_2 + \sqrt{\gamma_{1,k}} b_{1,\rm in} - \sqrt{\gamma_{2,k}} b_{2,\rm in}}{i\Delta_k + \frac{\gamma_a}{2}}. \tag{D8}$$

Combing Eqs. (D7) and (D8), we obtain

$$c_1 = -\sum_{k=1}^{N} \frac{\frac{1}{2}\gamma_{1,k} c_1 - \frac{1}{2}\sqrt{\gamma_{1,k}\gamma_{2,k}} c_2 + \gamma_{1,k} b_{1,\rm in} - \sqrt{\gamma_{1,k}\gamma_{2,k}} b_{2,\rm in}}{i\Delta_k + \frac{\gamma_a}{2}}, \tag{D9}$$

$$c_2 = -\sum_{k=1}^{N} \frac{-\frac{1}{2}\sqrt{\gamma_{1,k}\gamma_{2,k}} c_1 + \frac{1}{2}\gamma_{2,k} c_2 - \sqrt{\gamma_{1,k}\gamma_{2,k}} b_{1,\rm in} + \gamma_{2,k} b_{2,\rm in}}{i\Delta_k + \frac{\gamma_a}{2}}. \tag{D10}$$

The solutions of c_1 and c_2 reads

$$c_1 = \frac{-\left[\left(1+\frac{1}{2}\sum_{k=1}^{N}\frac{\gamma_{2,k}}{i\Delta_k+\frac{\gamma_a}{2}}\right)\left(\sum_{k=1}^{N}\frac{\gamma_{1,k}}{i\Delta_k+\frac{\gamma_a}{2}}\right)-\frac{1}{2}\left(\sum_{k=1}^{N}\frac{\sqrt{\gamma_{1,k}\gamma_{2,k}}}{i\Delta_k+\frac{\gamma_a}{2}}\right)^2\right]b_{1,\mathrm{in}}+\left(\sum_{k=1}^{N}\frac{\sqrt{\gamma_{1,k}\gamma_{2,k}}}{i\Delta_k+\frac{\gamma_a}{2}}\right)b_{2,\mathrm{in}}}{\left(1+\frac{1}{2}\sum_{k=1}^{N}\frac{\gamma_{1,k}}{i\Delta_k+\frac{\gamma_a}{2}}\right)\left(1+\frac{1}{2}\sum_{k=1}^{N}\frac{\gamma_{2,k}}{i\Delta_k+\frac{\gamma_a}{2}}\right)-\left(\frac{1}{2}\sum_{k=1}^{N}\frac{\sqrt{\gamma_{1,k}\gamma_{2,k}}}{i\Delta_k+\frac{\gamma_a}{2}}\right)^2}, \tag{D11}$$

$$c_2 = \frac{\left(\sum_{k=1}^{N}\frac{\sqrt{\gamma_{1,k}\gamma_{2,k}}}{i\Delta_k+\frac{\gamma_a}{2}}\right)b_{1,\mathrm{in}}-\left[\left(1+\frac{1}{2}\sum_{k=1}^{N}\frac{\gamma_{1,k}}{i\Delta_k+\frac{\gamma_a}{2}}\right)\left(\sum_{k=1}^{N}\frac{\gamma_{2,k}}{i\Delta_k+\frac{\gamma_a}{2}}\right)-\frac{1}{2}\left(\sum_{k=1}^{N}\frac{\sqrt{\gamma_{1,k}\gamma_{2,k}}}{i\Delta_k+\frac{\gamma_a}{2}}\right)^2\right]b_{2,\mathrm{in}}}{\left(1+\frac{1}{2}\sum_{k=1}^{N}\frac{\gamma_{1,k}}{i\Delta_k+\frac{\gamma_a}{2}}\right)\left(1+\frac{1}{2}\sum_{k=1}^{N}\frac{\gamma_{2,k}}{i\Delta_k+\frac{\gamma_a}{2}}\right)-\left(\frac{1}{2}\sum_{k=1}^{N}\frac{\sqrt{\gamma_{1,k}\gamma_{2,k}}}{i\Delta_k+\frac{\gamma_a}{2}}\right)^2}. \tag{D12}$$

Similarily, the input-output relations can be readily obtained by inserting c_1 and c_2 into Eqs. (A15)-(A16).

[1] X. Gu, A. F. Kockum, A. Miranowicz, Y.-x. Liu, and F. Nori, Microwave photonics with superconducting quantum circuits, Phys. Rep. **718-719**, 1 (2017).

[2] A. Blais, R.-S. Huang, A. Wallraff, S. M. Girvin, and R. J. Schoelkopf, Cavity quantum electrodynamics for superconducting electrical circuits: An architecture for quantum computation, Phys. Rev. A **69**, 062320 (2004).

[3] A. Wallraff, D. I. Schuster, A. Blais, L. Frunzio, R.-S. Huang, J. Majer, S. Kumar, S. M. Girvin, and R. J. Schoelkopf, Strong coupling of a single photon to a superconducting qubit using circuit quantum electrodynamics, Nature **431**, 162 (2004).

[4] J.-T. Shen and S. Fan, Coherent single photon transport in a one-dimensional waveguide coupled with superconducting quantum bits, Phys. Rev. Lett. **95**, 213001 (2005); J. T. Shen and S. Fan, Coherent photon transport from spontaneous emission in one-dimensional waveguides, Opt. Lett. **30**, 2001 (2005).

[5] V. Bužek, G. Drobný, M. G. Kim, M. Havukainen, and P. L. Knight, Numerical simulations of atomic decay in cavities and material media, Phys. Rev. A **60**, 582 (1999).

[6] L. Zhou, Z. R. Gong, Y.-x. Liu, C. P. Sun, and F. Nori, Controllable scattering of a single photon inside a one-dimensional resonator waveguide, Phys. Rev. Lett. **101**, 100501 (2008).

[7] J.-T. Shen and S. Fan, Theory of single-photon transport in a single-mode waveguide. I. Coupling to a cavity containing a two-level atom, Phys. Rev. A **79**, 023837 (2009); Theory of single-photon transport in a single-mode waveguide. II. Coupling to a whispering-gallery resonator containing a two-level atom, Phys. Rev. A **79**, 023838 (2009).

[8] O. Astafiev, A. M. Zagoskin, A. A. Abdumalikov, Y. A. Pashkin, T. Yamamoto, K. Inomata, Y. Nakamura, and J. S. Tsai, Resonance fluorescence of a single artificial atom, Science **327**, 840 (2010).

[9] J.-Q. Liao and C. K. Law, Correlated two-photon transport in a one-dimensional waveguide side-coupled to a nonlinear cavity, Phys. Rev. A **82**, 053836 (2010).

[10] D. Zueco, J. J. Mazo, E. Solano, and J. J. García-Ripoll, Microwave photonics with josephson junction arrays: Negative refraction index and entanglement through disorder, Phys. Rev. B **86**, 024503 (2012).

[11] K. Lalumière, B. C. Sanders, A. F. van Loo, A. Fedorov, A. Wallraff, and A. Blais, Input-output theory for waveguide qed with an ensemble of inhomogeneous atoms, Phys. Rev. A **88**, 043806 (2013).

[12] A. F. van Loo, A. Fedorov, K. Lalumiere, B. C. Sanders, A. Blais, and A. Wallraff, Photon-mediated interactions between distant artificial atoms, Science **342**, 1494 (2013).

[13] H. Pichler and P. Zoller, Photonic circuits with time delays and quantum feedback, Phys. Rev. Lett. **116**, 093601 (2016).

[14] J.-F. Huang, J.-Q. Liao, and C. P. Sun, Photon blockade induced by atoms with rydberg coupling, Phys. Rev. A **87**, 023822 (2013).

[15] Q. Li, L. Zhou, and C. P. Sun, Waveguide quantum electrodynamics: Controllable channel from quantum interference, Phys. Rev. A **89**, 063810 (2014).

[16] X. Gu, S.-N. Huai, F. Nori, and Y.-x. Liu, Polariton states in circuit qed for electromagnetically induced transparency, Phys. Rev. A **93**, 063827 (2016).

[17] J. Long, H. S. Ku, X. Wu, X. Gu, R. E. Lake, M. Bal, Y.-x. Liu, and D. P. Pappas, Electromagnetically induced transparency in circuit quantum electrodynamics with nested polariton states, Phys. Rev. Lett. **120**, 083602 (2018).

[18] W. Nie, Z. H. Peng, F. Nori, and Y.-x. Liu, Topologically protected quantum coherence in a superatom, Phys. Rev. Lett. **124**, 023603 (2020).

[19] W. Nie and Y.-x. Liu, Bandgap-assisted quantum control of topological edge states in a cavity, Phys. Rev. Research **2**, 012076 (2020).

[20] S. Fan, Sharp asymmetric line shapes in side-coupled waveguide-cavity systems, Appl. Phys. Lett. **80**, 908 (2002).

[21] A. Chiba, H. Fujiwara, J.-i. Hotta, S. Takeuchi, and K. Sasaki, Fano resonance in a multimode tapered fiber coupled with a microspherical cavity, Appl. Phys. Lett. **86**, 261106 (2005).

[22] P. Chak, S. Pereira, and J. E. Sipe, Coupled-mode theory for periodic side-coupled microcavity and photonic crystal structures, Phys. Rev. B **73**, 035105 (2006).

[23] Y.-F. Xiao, M. Li, Y.-C. Liu, Y. Li, X. Sun, and Q. Gong, Asymmetric fano resonance analysis in indirectly coupled microresonators, Phys. Rev. A **82**, 065804 (2010).

[24] S. Longhi, Tunable dynamic fano resonances in coupled-

resonator optical waveguides, Phys. Rev. A **91**, 063809 (2015).
[25] S. John and J. Wang, Quantum optics of localized light in a photonic band gap, Phys. Rev. B **43**, 12772 (1991).
[26] M. Notomi, K. Yamada, A. Shinya, J. Takahashi, C. Takahashi, and I. Yokohama, Extremely large group-velocity dispersion of line-defect waveguides in photonic crystal slabs, Phys. Rev. Lett. **87**, 253902 (2001); M. Notomi, E. Kuramochi, and T. Tanabe, Large-scale arrays of ultrahigh-q coupled nanocavities, Nat. Photon. **2**, 741 (2008).
[27] M. F. Yanik and S. Fan, Stopping light all optically, Phys. Rev. Lett. **92**, 083901 (2004); M. F. Yanik, W. Suh, Z. Wang, and S. Fan, Stopping light in a waveguide with an all-optical analog of electromagnetically induced transparency, Phys. Rev. Lett. **93**, 233903 (2004); M. F. Yanik and S. Fan, Stopping and storing light coherently, Phys. Rev. A **71**, 013803 (2005).
[28] Q. Xu, P. Dong, and M. Lipson, Breaking the delay-bandwidth limit in a photonic structure, Nat. Phys. **3**, 406 (2007).
[29] Y. Dumeige, S. Trebaol, and P. Féron, Intracavity coupled-active-resonator-induced dispersion, Phys. Rev. A **79**, 013832 (2009).
[30] D. D. Smith, H. Chang, K. A. Fuller, A. T. Rosenberger, and R. W. Boyd, Coupled-resonator-induced transparency, Phys. Rev. A **69**, 063804 (2004).
[31] K. Totsuka, N. Kobayashi, and M. Tomita, Slow light in coupled-resonator-induced transparency, Phys. Rev. Lett. **98**, 213904 (2007).
[32] Y.-F. Xiao, X.-B. Zou, W. Jiang, Y.-L. Chen, and G.-C. Guo, Analog to multiple electromagnetically induced transparency in all-optical drop-filter systems, Phys. Rev. A **75**, 063833 (2007).
[33] X. Yang, M. Yu, D.-L. Kwong, and C. W. Wong, All-optical analog to electromagnetically induced transparency in multiple coupled photonic crystal cavities, Phys. Rev. Lett. **102**, 173902 (2009).
[34] E. N. Bulgakov and A. F. Sadreev, Bound states in the continuum in photonic waveguides inspired by defects, Phys. Rev. B **78**, 075105 (2008).
[35] T. Shi and C. P. Sun, Lehmann-symanzik-zimmermann reduction approach to multiphoton scattering in coupled-resonator arrays, Phys. Rev. B **79**, 205111 (2009).
[36] P. Longo, P. Schmitteckert, and K. Busch, Few-photon transport in low-dimensional systems: Interaction-induced radiation trapping, Phys. Rev. Lett. **104**, 023602 (2010).
[37] M. Biondi, S. Schmidt, G. Blatter, and H. E. Türeci, Self-protected polariton states in photonic quantum metamaterials, Phys. Rev. A **89**, 025801 (2014).
[38] A. Biella, L. Mazza, I. Carusotto, D. Rossini, and R. Fazio, Photon transport in a dissipative chain of nonlinear cavities, Phys. Rev. A **91**, 053815 (2015).
[39] L. Qiao and C.-P. Sun, Atom-photon bound states and non-markovian cooperative dynamics in coupled-resonator waveguides, Phys. Rev. A **100**, 063806 (2019).
[40] N. M. Sundaresan, R. Lundgren, G. Zhu, A. V. Gorshkov, and A. A. Houck, Interacting qubit-photon bound states with superconducting circuits, Phys. Rev. X **9**, 011021 (2019).
[41] S. Fan, i. m. c. E. Kocabaş, and J.-T. Shen, Input-output formalism for few-photon transport in one-dimensional nanophotonic waveguides coupled to a qubit, Phys. Rev. A **82**, 063821 (2010); S. Xu and S. Fan, Input-output formalism for few-photon transport: A systematic treatment beyond two photons, Phys. Rev. A **91**, 043845 (2015).
[42] A. Yariv, Y. Xu, R. K. Lee, and A. Scherer, Coupled-resonator optical waveguide: a proposal and analysis, Opt. Lett. **24**, 711 (1999); Y. Xu, Y. Li, R. K. Lee, and A. Yariv, Scattering-theory analysis of waveguide-resonator coupling, Phys. Rev. E **62**, 7389 (2000).
[43] M. Pierre, S. R. Sathyamoorthy, I.-M. Svensson, G. Johansson, and P. Delsing, Resonant and off-resonant microwave signal manipulation in coupled superconducting resonators, Phys. Rev. B **99**, 094518 (2019).
[44] J. Leppäkangas, J. D. Brehm, P. Yang, L. Guo, M. Marthaler, A. V. Ustinov, and M. Weides, Resonance inversion in a superconducting cavity coupled to artificial atoms and a microwave background, Phys. Rev. A **99**, 063804 (2019).
[45] Q.-M. Chen, The scattering coefficients of superconducting microwave resonators: I. Transfer-matrix approach, (2021).
[46] M. J. Collett and C. W. Gardiner, Squeezing of intracavity and traveling-wave light fields produced in parametric amplification, Phys. Rev. A **30**, 1386 (1984).
[47] C. W. Gardiner and M. J. Collett, Input and output in damped quantum systems: Quantum stochastic differential equations and the master equation, Phys. Rev. A **31**, 3761 (1985).
[48] H. J. Carmichael, *Statistical methods in quantum optics 1: master equations and Fokker-Planck equations* (Springer Science & Business Media, 2013).
[49] S. M. Girvin, Circuit QED: superconducting qubits coupled to microwave photons, in *Quantum Machines: Measurement and Control of Engineered Quantum Systems*, edited by M. Devoret, B. Huard, R. Schoelkopf, and L. F. Cugliandolo (Oxford University Press, 2011) pp. 113–256.
[50] G. Breit and E. Wigner, Capture of slow neutrons, Phys. Rev. **49**, 519 (1936).
[51] A. E. Miroshnichenko, S. Flach, and Y. S. Kivshar, Fano resonances in nanoscale structures, Rev. Mod. Phys. **82**, 2257 (2010).
[52] M. Fischer, Q.-M. Chen, C. Besson, P. Eder, J. Goetz, S. Pogorzalek, M. Renger, E. Xie, M. J. Hartmann, K. G. Fedorov, A. Marx, F. Deppe, and R. Gross, In situ tunable nonlinearity and competing signal paths in coupled superconducting resonators, Phys. Rev. B **103**, 094515 (2021).
[53] A. Wójcik, T. Łuczak, P. Kurzyński, A. Grudka, T. Gdala, and M. Bednarska, Unmodulated spin chains as universal quantum wires, Phys. Rev. A **72**, 034303 (2005); Multiuser quantum communication networks, Phys. Rev. A **75**, 022330 (2007).
[54] J.-Q. Liao, J.-F. Huang, Y.-x. Liu, L.-M. Kuang, and C. P. Sun, Quantum switch for single-photon transport in a coupled superconducting transmission-line-resonator array, Phys. Rev. A **80**, 014301 (2009).
[55] J.-Q. Liao, Z. R. Gong, L. Zhou, Y.-x. Liu, C. P. Sun, and F. Nori, Controlling the transport of single photons by tuning the frequency of either one or two cavities in an array of coupled cavities, Phys. Rev. A **81**, 042304 (2010).
[56] M. Sumetsky and B. Eggleton, Modeling and

optimization of complex photonic resonant cavity circuits, Opt. Express **11**, 381 (2003).

[57] Y. Hara, T. Mukaiyama, K. Takeda, and M. Kuwata-Gonokami, Heavy photon states in photonic chains of resonantly coupled cavities with supermonodispersive microspheres, Phys. Rev. Lett. **94**, 203905 (2005).

[58] D. O'Brien, M. D. Settle, T. Karle, A. Michaeli, M. Salib, and T. F. Krauss, Coupled photonic crystal heterostructure nanocavities, Opt. Express **15**, 1228 (2007).

[59] D. F. Walls and G. J. Milburn, Effect of dissipation on quantum coherence, Phys. Rev. A **31**, 2403 (1985).

[60] C. W. Gardiner and P. Zoller, *Quantum noise: a handbook of Markovian and non-Markovian quantum stochastic methods with applications to quantum optics*, second enlarged ed. (Springer, 2000).

[61] Q. A. Turchette, C. J. Myatt, B. E. King, C. A. Sackett, D. Kielpinski, W. M. Itano, C. Monroe, and D. J. Wineland, Decoherence and decay of motional quantum states of a trapped atom coupled to engineered reservoirs, Phys. Rev. A **62**, 053807 (2000).

[62] C. J. Myatt, B. E. King, Q. A. Turchette, C. A. Sackett, D. Kielpinski, W. M. Itano, C. Monroe, and D. J. Wineland, Decoherence of quantum superpositions through coupling to engineered reservoirs, Nature **403**, 269 (2000).

[63] Y.-x. Liu, i. m. c. K. Özdemir, A. Miranowicz, and N. Imoto, Kraus representation of a damped harmonic oscillator and its application, Phys. Rev. A **70**, 042308 (2004).

[64] A. Megrant, C. Neill, R. Barends, B. Chiaro, Y. Chen, L. Feigl, J. Kelly, E. Lucero, M. Mariantoni, P. J. J. O'Malley, D. Sank, A. Vainsencher, J. Wenner, T. C. White, Y. Yin, J. Zhao, C. J. Palmstrøm, J. M. Martinis, and A. N. Cleland, Planar superconducting resonators with internal quality factors above one million, Appl. Phys. Lett. **100**, 113510 (2012).

[65] C. W. Gardiner, Driving a quantum system with the output field from another driven quantum system, Phys. Rev. Lett. **70**, 2269 (1993).